Body-wandering reveals an embodied dimension of thought with distinct affective and neural signatures

Leah Banellis*[1], Niia Nikolova[1], Malthe Brændholdt[1], Melina Vejlø[1], Francesca Fardo[1,2], Jonathan Smallwood[3], Micah G. Allen[1,4]

[1]Center of Functionally Integrative Neuroscience, Aarhus University, Denmark

[2]Danish Pain Research Center, Aarhus University, Denmark

[3]Queen's University, Ontario, Canada

[4]Cambridge Psychiatry, Cambridge, United Kingdom

Correspondence: Leah Banellis, leahbanellis@cfin.au.dk

Abstract

Humans often engage in self-generated thoughts when unoccupied by external events, a phenomenon commonly known as mind-wandering. Previous research has predominantly focused on the cognitive aspects of mind-wandering, overlooking the potential embodied or interoceptive components that contribute to our ongoing thought patterns. In this study, we addressed this gap by exploring "body-wandering"—thoughts related to internal bodily sensations such as breathing, heartbeat, and gastrointestinal functions. To assess body-wandering, we applied a retrospective multi-dimensional interoceptive experience sampling approach in 536 healthy participants concurrently with resting-state functional brain imaging. Our findings revealed that body-wandering is distinct from cognitively focused thoughts, underscoring the unique role of embodied processes in ongoing experience. Embodied thought patterns were associated with increased negative affect, heightened physiological arousal, and reduced ADHD symptoms. In contrast, cognitive-focused thoughts were linked to decreased negative affect, lower arousal, and higher depression symptoms. Notably, body-wandering corresponded with a unique neural signature involving increased connectivity between somatomotor, interoceptive, and thalamocortical brain networks. These results emphasise the importance of incorporating embodied processes into theoretical models of mind-wandering and suggest that individual differences in body-wandering significantly impact emotional states and mental health.

Keywords: mind-wandering, interoception, emotion, brain connectivity, mental health.

Significance statement

Contemporary cognitive neuroscience recognizes the role of internally generated states known as mind-wandering. However, research has predominantly taken a cognitive perspective, overlooking the embodied influences on conscious experience. Our study addresses this gap by demonstrating the unique contribution of body-related and interoceptive thoughts to waking cognition. This "body-wandering" was associated with increased negative affect, heightened physiological arousal, and reduced ADHD symptoms, along with a distinct neural signature involving interoceptive, somatomotor, and subcortical networks. Conversely, cognitive mind-wandering was linked to decreased negative affect, lower arousal, and increased depressive symptoms. Incorporating embodied processes into models of mind-wandering provides a more comprehensive theoretical framework and reveals how these experiences influence our emotional state and mental health.

Introduction

The human mind is a ceaseless wanderer, with ongoing thought constantly shifting between self-generated thoughts and externally directed experiences (Christoff et al., 2016; Smallwood & Schooler, 2015). While research on patterns of ongoing thoughts has flourished in recent years (Smallwood et al., 2021), studies have largely focused on cognitive features of experience and so have neglected the possibility that embodied processes can influence our thought experiences. In this study, we address this theoretical gap in our understanding of ongoing thought by establishing the concept of interoceptive "body-wandering" - thoughts and sensations related to our internal bodily state - and investigate its affective, physiological, and neural correlates during a period of wakeful rest.

Ongoing thought patterns are recognised to be multifaceted, with contemporary work highlighting that they can reflect incoming sensory information, such as when we watch movies (Wallace et al., 2024), and maintain detailed information regarding tasks we perform either in the lab (Mckeown et al., 2023) or during periods of work in daily life (Mckeown et al., 2021; Mulholland et al., 2023). Ongoing thought patterns can also reflect self-generated processes that allow for creativity and innovative problem solving (Gable et al., 2019), however, they can also precipitate intrusive unpleasant features that are linked to problems in mental health such as with depressive rumination (Killingsworth & Gilbert, 2010; Mulholland et al., 2023). Psychopathological consequences of ongoing thoughts also include associations with ADHD (Biederman et al., 2019; Bozhilova et al., 2018; Lanier et al., 2021). Emerging evidence indicates that difficulties in patterns of ongoing thought in individuals with ADHD may stem from dysfunctions in the locus coeruleus-norepinephrine (LC-NE) system, a neural system critical for regulating arousal and attention (Bellato et al., 2020, 2023; Martella et al., 2020). Dysregulation in the LC-NE system can lead to a predisposition towards hypoarousal, which may contribute to the characteristic symptoms of ADHD, including inattentiveness and disrupted thought patterns. Supporting this notion, individuals with ADHD have reduced vagally mediated heart rate variability (high-frequency power) than controls (Bellato et al., 2023; Robe et al., 2019), indicating decreased parasympathetic activity and altered autonomic nervous system regulation.

While internally generated contributions to ongoing thought are now a well-documented feature of human experience, they often focus primarily on cognitive features of experience, neglecting the possibility that experiences can have important embodied features. This oversight is especially important given the mounting evidence for an interoceptive component of emotional experience and mental health (Critchley & Garfinkel, 2017; Khalsa et al., 2018). An over focus on cognitive features of ongoing thought has important implications for theoretical perspectives on ongoing thought patterns (Smallwood et al., 2021). For example, brain regions implicated in cognitive aspects of experience include areas associated with executive control, such as the dorsolateral prefrontal cortex (Turnbull et al., 2019), and areas involved in autobiographical memory, such as the medial prefrontal cortex (Konu et al., 2020). In contrast, the possibility that

ongoing thought patterns can have embodied features raises the possibility that brain regions involved in interoception, somatosensation and action may also contribute to ongoing experience even when we are unoccupied by an external task.

Consistent with the possibility that embodied processes contribute to our ongoing thought processes, there are important similarities between the neural mechanisms of interoception and those linked to cognitive features of ongoing thought, including both regions of the default mode and saliency networks. For example, the posterior cingulate cortex and precuneus activate with interoceptive processing during various forms of self-related cognition (Babo-Rebelo et al., 2019; Babo-Rebelo, Richter, et al., 2016; Babo-Rebelo, Wolpert, et al., 2016; Park et al., 2018). These regions are a core part of the default mode network, with the medial prefrontal cortex and inferior parietal lobules, which are implicated in ongoing thought (Christoff et al., 2009; Fox et al., 2015; Greicius et al., 2003; Raichle et al., 2001). Consistent with this possibility, the discovery of an "interoceptive and allostatic" brain network has been reported, with key nodes situated both within the default mode and salience networks (Barrett & Simmons, 2015; Kleckner et al., 2017). Notably, recent perspectives on waking cognitive experiences at rest are known to depend on the interaction between the default mode and saliency networks, as well as to the dorsal attention network (Hardikar et al., 2024; Turnbull et al., 2019). Our study, therefore, explored the possibility that ongoing thought patterns that reflect attention to our body and its sensations depend on a combination of regions that play an established role in ongoing thought processes, as well as those that are linked directly to interoception.

To address the gap in our understanding of how embodied processes contribute to ongoing thought experiences, we probed interoceptive, affective, and cognitive contents of thoughts that occur during wakeful rest. We expanded the multi-dimensional experience sampling (mDES) approach to also probe the interoceptive and embodied dimension of ongoing thought experiences. These were administered following a period of wakeful rest while brain activity was recorded using functional magnetic resonance imaging (fMRI). In addition to the neural and experiential characteristics of "body-wandering" and "cognitive-wandering", we also sought to identify their affective and physiological correlates. With this data, we hoped to address the scientific gap in understanding how embodied processes contribute to our experience, and thereby improve theoretical accounts of the brain and the experiential basis of the ongoing thought patterns that play a central role in our conscious experiences.

Results

Item level analyses

We expanded upon the established approach of assessing affective and cognitive mind-wandering by probing interoceptive and embodied content, using a multidimensional interoceptive experience sampling (MDIES) approach, with the aim of characterising the extent of body-related versus more traditional cognitive dimensions of mind-wandering. To assess these

dimensions, we first calculated indices of cognitive and interoceptive thoughts by averaging the embodied and cognitive items separately (see Methods Mind-Wandering Summaries for the body average and cognitive average details and see Figure 1 (Right)). We found that interoceptive thoughts were reported less frequently overall than typical cognitive content. This is supported by a significant Wilcoxon signed-rank test comparing embodied and cognitive item averages (body item average: Median (Mdn) = 36.5, Range = 0-79.2, cognitive item average: Mdn = 47.1, Range = 3.8-100; W(535) = 39209, *p* <.001, rB = -0.455). Within the body-related items, non-specific thoughts about bodily movement were significantly more prevalent than all interoceptive thoughts of specific organs, with the exception of movement with breathing-related thoughts which was not significant but followed the same pattern (Wilcoxon signed rank tests W range = 75063 to 101878, *p range* = .002 to <.001, rB range = 0.157 to 0.667, see Supplementary Table 1). Respiration (i.e., thoughts about breathing) was the most dominant of the interoceptive mind-wandering content (see Figure 1 (Left)).

While most participants reported a positive emotional experience during rest, there was substantial variability in individual affective tone (negative difference score: Neg - Pos Mdn = -15.820, Range = -100 to 100). Interestingly, interoceptive body-wandering correlated with an increase in negative thoughts, and compatibly, a reduction in positive affective content. Specifically, the following body-related items significantly correlated with less positive thoughts: arousal, heart, bladder, skin, and stomach (rs range = -0.175 to -0.298, *pFDR range = all* <.001). Correspondingly the subsequent embodied items were significantly associated with heightened negative content: body, breath, heart, bladder, skin, and stomach (rs range = 0.118 to 0.225, *pFDR range* = .012 to <.001). Despite this, spontaneous thoughts concerning movement significantly correlated with more positive thoughts (rs = 0.102, *pFDR* = .030) (see Supplementary Table 2 for body-affect item correlation statistics). All correlations persisted when controlling for age, gender and body mass index (BMI) (see Supplementary Figure 1). Therefore, thoughts about the body and interoceptive sensations are overall related to negative affective ongoing thought (see Figure 1 (Middle)).

In the opposing direction, items reflecting cognitive (past, future, other, self) or descriptive (image, distant, focus, vague, ruminate, vivid) aspects of mind-wandering demonstrated more positive (rs range = 0.097 to 0.305, pFDR range = .049 to <.001) and/or less negative ongoing thoughts (rs = -0.140 to -0.218, pFDR range = .004 to < .001) (see Supplementary Figure 2 for full item correlation statistics, including partial correlations controlling for age, gender, and BMI). Thus, body-related and cognitive aspects of mind-wandering have an anti-correlated relationship with emotional thought experiences.

Figure 1: Ongoing thought item ratings including body-related, cognitive, and affective content (MDIES) after resting state MRI.

(Left) Boxplots of MDIES item ratings (pink: body-related items and blue: classical cognitive/affective items). (Middle) Spearman correlation analysis of affect and body-related mind-wandering items (yellow: body-related items correlations with the positive mind-wandering item, purple: body-related items correlations with the negative mind-wandering item, asterisks indicate FDR corrected significant correlations). (Right) Word clouds of the mind-wandering summary scores (from top to bottom: body-wandering average, cognitive-wandering average, and negative-positive difference score) correlations with individual items to highlight the contribution of each item to the respective summary score (size of the word demonstrates the magnitude of the correlation, and colour the polarity as shown via the colour bars).

Psychological network analysis

We next conducted a network analysis to identify structural patterns and relationships among items reflecting mind-wandering experiences. This revealed a network of 21 nodes-each representing a specific mind-wandering item-with 58 non-zero connections (out of 210 possible edges). This analysis also included the evaluation of the most central and influential individual items. For example, positive mind-wandering emerged as the most central node, exhibiting the strongest direct connections (strength centrality), the most indirect connections (closeness centrality), and the most active as a crucial intermediary between other nodes (betweenness centrality i.e., shortest path to other nodes). Detailed mind-wandering (vague), and bladder-related thoughts were also highly central, suggesting these facets of mind-wandering are highly relevant for other aspects of ongoing thought. In contrast, words, movement, and breath-related

thoughts were the least central nodes with respect to overall interactions with other dimensions of ongoing thought. Furthermore, past-oriented mind-wandering was expected to be the most influential when considering the sign of the direct connections to other nodes, while ruminating thoughts the least influential (see Figure 2 and Supplementary Figure 3 for network centrality indices).

The most prominent negative and positive edge weights involved connections between positive-negative (-0.300), vague-image (0.229), heart-bladder (0.165), positive-bladder (-0.156), and bladder-vague (-0.143) nodes. This highlights the strongest correlations between pairs of mind-wandering dimensions, exhibiting important relations among affective, embodied and the detailed nature of ongoing thought. To assess the robustness and stability of the overall network, we also performed bootstrapped analysis (2500 repetitions) of the confidence intervals for the estimated edge weights, and of the correlation stability coefficients of the centrality indices. This showed that although large edge-weight confidence intervals indicate high variability in edge weight estimation (see Supplementary Figure 4), the stability coefficients for each centrality index were relatively stable (all exceeded 0.5, see Supplementary Figure 5). For significant edges and centrality index significance, please refer to the Supplementary Figures 6-10.

Next, to identify subclusters or communities of nodes within the overall thought network, we applied a spinglass community detection algorithm. This data-driven approach identified 5 communities of nodes. Interestingly, this discovered a subnetwork community of body-related nodes with negative affect. This body-wandering subnetwork included most of the interoceptive body items except for thoughts regarding the breath, which clustered with temporality (past/future thoughts) and the vague or focused nature of visual thoughts. Content concerning the overall body and thoughts of movement formed a small subnetwork. Finally, the temporal distance and vivid nature of thoughts formed a small subnetwork and positive affect clustered in a subnetwork community with thoughts concerning personhood, verbal and ruminating content.

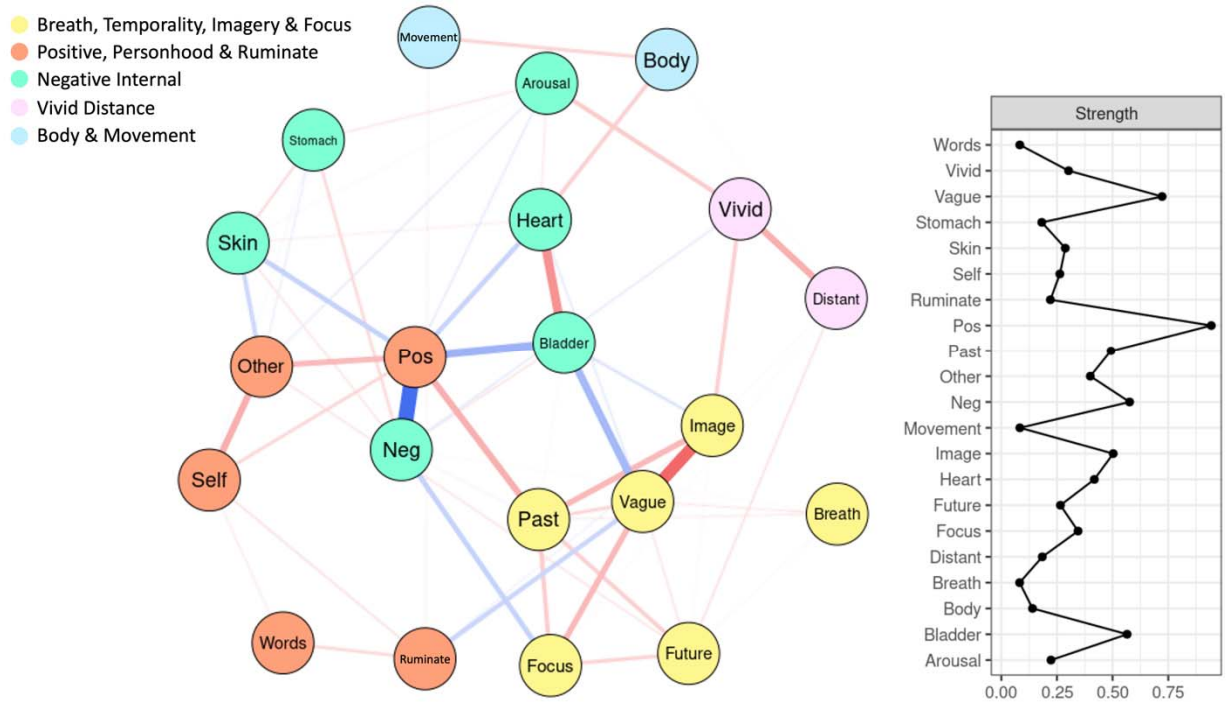

Figure 2: Network Analysis of MDIES Items.

(Left) EPICglasso network analysis of partial correlations between ongoing thought items (MDIES). Blue edges represent negative partial correlations between two nodes and red edges show positive partial correlations. Thickness of the edge represents the association magnitude. Nodes are colour coded by the 5 communities detected via the spinglass community detection algorithm. (Right) Strength of each node representing the most direct connections for each item.

Mental health individual differences

Mind-wandering has been extensively related to psychopathology and mental health, particularly in the domains of ADHD and depression. We examined the associations between symptoms of ADHD and depression with embodied (body-wandering), cognitive, and negative mind-wandering constructs. ADHD symptoms were assessed via the Adult ADHD Self-Report Scale (ASRS) (Kessler et al., 2005), while depressive symptoms were measured via the Major Depression Inventory (MDI) (Bech et al., 2015) (see methods mental health assessment section for scoring details).

Body-wandering ratings were significantly negatively correlated with ADHD and depressive symptoms (ADHD: rs = -0.138, *pFDR* = .003, depression: rs = -0.132, *pFDR* = .004). Contrastingly, cognitive-wandering was significantly positively correlated with ADHD and depressive symptoms (ADHD: rs = 0.143, *pFDR* = .003, depression: rs = 0.156, *pFDR* < .001) (see Figure 3 and Supplementary Table 3). These correlations persisted when partialling out age, gender, and BMI (see Supplementary Figure 11). A backward stepwise multiple linear regression

incorporating both ADHD and depression symptoms as predictors of body-wandering to control for symptom comorbidity, indicated that only ADHD significantly predicted body-wandering scores (b = -0.120, t = -2.718, p = .007; R^2 = 0.014, F(1,507) = 7.389, p = .007), while depression was not retained in the final model. In contrast, in the model predicting cognitive-wandering, only depressive symptoms were significant predictors (b = 4.853, t = 3.920, p < .001; R^2 = 0.029, F(1,507) = 15.366, p = < .001), while ADHD was not retained in the final model (See Supplementary Figure 12). These findings suggest that ADHD and depression have distinct relationships with ongoing thoughts patterns: ADHD symptoms are associated with reduced body-wandering, while depressive symptoms are associated with increased cognitive-wandering.

Post-hoc analyses examining correlations between ADHD symptoms and individual items from the body and cognitive-wandering scales (i.e., MDIES items) revealed that mind-wandering about the heart had the strongest negative correlation with ADHD symptoms (rs = -0.211, *pFDR* < .001), followed by thoughts regarding the bladder (rs = -0.106, *pFDR* = .035), and the skin (rs = -0.104, *pFDR* = .038). For depressive symptoms, temporal mind-wandering about the past (rs = 0.164, *pFDR* < .001) and future (rs = 0.123, *pFDR* = .014) contributed most to the association with cognitive-wandering (see Supplementary Figure 13). Intriguingly, depressive symptoms also correlated with less negative mind-wandering (negative difference score: rs = -0.098, *pFDR* = 0.047). Post-hoc correlations suggested this was driven by a weak positive correlation between depressive symptoms and positive affective mind-wandering (rs = 0.094, *pFDR* = 0.049).

Physiological individual differences

We also evaluated the influence of individual differences in interoceptive physiology (cardiac, respiratory, and gastric metrics) on embodied and cognitive-wandering (see Methods Physiological Measurements section). Body-wandering significantly correlated with a higher heart rate, higher sympathovagal balance (LF/HF ratio), lower parasympathetic heart rate variability (RMSSD, high frequency power), as well as a higher mean respiratory depth, higher variability in both respiratory depth and duration, and a higher gastric maximum power in normal gastric range (normogastria). Contrastingly, in the opposing direction to body-wandering, we observed cognitive-wandering correlations with higher parasympathetic heart rate variability (RMSSD, high frequency power), lower sympathovagal balance (LF/HF ratio), lower mean and variability of respiratory depth, and lower normogastric maximum power (see Figure 3 and Supplementary Table 3 for full physiological mind-wandering correlation statistics). Importantly, these correlations persisted even when controlling for age, gender, and BMI (see Supplementary Figure 11).

A backward stepwise multiple linear regression including the significant physiological metrics from the body-wandering correlations as predictors, indicated a final model with RMSSD, mean respiratory depth, respiratory duration variability, and normogastric maximum power as significantly predicting body-wandering (R^2 = 0.150, F(4,239) = 10.565, p = < .001). Similarly,

RMSSD, mean respiratory depth, and normogastric maximum power were retained from a backward stepwise regression with cognitive-wandering (R^2 = 0.164, F(3,242) = 15.814, p = < .001) (see Supplementary Figure 14).

We conducted post-hoc correlations of physiological metrics with individual MDIES items. The highest physiological correlation with body-wandering was skin-related thoughts with RMSSD heart rate variability (rs = -0.237, pFDR < .001), and with mean respiration depth (rs = 0.233, pFDR < .001). Whereas, the highest correlation between cognitive-wandering and physiological measures were mean respiration depth with past-oriented thoughts (rs = -0.216, pFDR < .001) (see Supplementary Figure 15 for all post-hoc physiology correlations).

Finally, negative affective mind-wandering significantly correlated with an increased heart rate, LF/HF ratio, respiratory depth (mean and variability), and decreased parasympathetic heart rate variability (high frequency power and RMSSD) (see Supplementary Table 3).

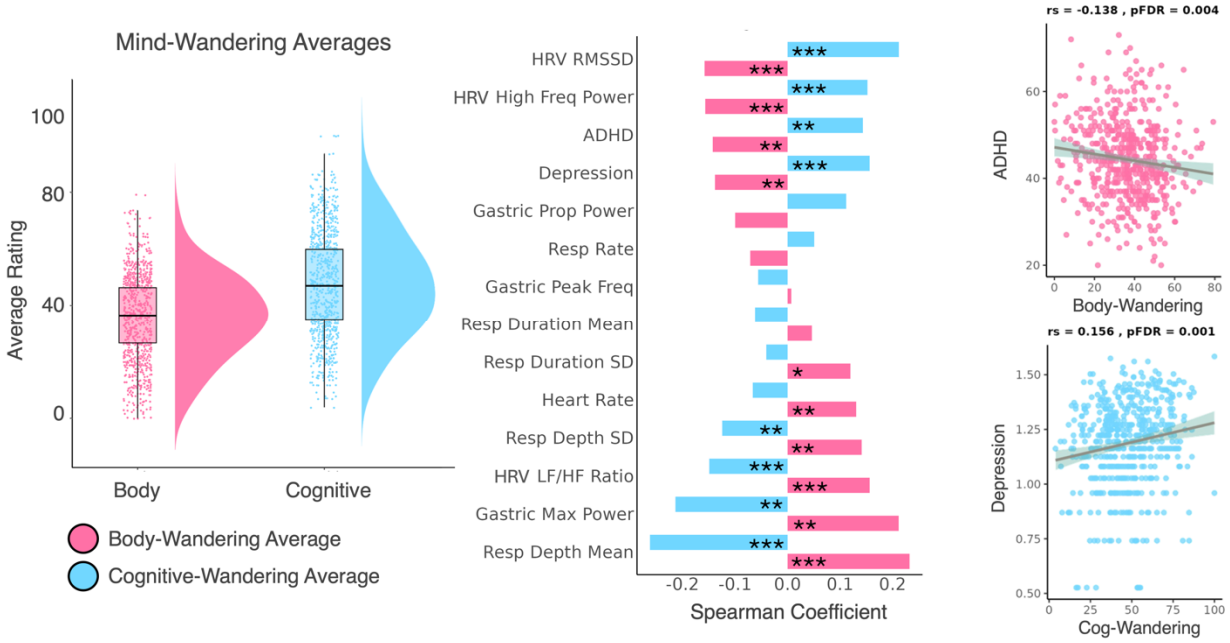

Figure 3: Body-wandering and cognitive-wandering averages, and their relationship with mental health symptoms and physiology.

(Left) Raincloud plot of mind-wandering averages representing overall body-wandering and cognitive-wandering (pink: average of body-related items and blue: average of cognitive-wandering items). (Middle) Full Spearman correlation analysis of body/cognitive-wandering with mental health symptoms (ADHD and depression) and physiological metrics across cardiac (heart rate variability: RMSSD and high frequency power, sympathovagal balance: LF/HF ratio, and heart rate), respiratory (respiratory rate, respiratory duration mean, respiratory duration variability (SD), respiratory depth variability (SD), respiratory depth mean), and gastric systems

(gastric proportion of power, gastric peak frequency, gastric maximum power (all in normogastria), revealing an anticorrelated pattern of body-wandering in contrast to cognitive-wandering (asterisks indicate FDR corrected significant correlations). (Right) Correlations of body and cognitive-wandering averages with ADHD and depression symptoms.

Cortical fingerprints of body-wandering

To elucidate the neural correlates underlying embodied mind-wandering, we employed canonical correlation analysis (CCA) to identify resting-state connectivity patterns associated with interoceptive and cognitive thoughts. This analysis revealed a significant, cross-validated CCA mode that captures a neural fingerprint of interoceptive thoughts, characterized by heightened connectivity among interoceptive, somatomotor, and subcortical networks (canonical variate in-sample $r(293) = 0.386$; out-of-sample $r(194) = 0.354$; $p = 0.001$; robustness = 80%; see Supplementary Table 4). The highest canonical loadings, reflecting the strongest associations, were observed for embodied and negative affective thoughts, specifically sensations related to the stomach (loading = 0.576), physiological arousal (0.442), breathing (0.345), movement (0.300), and negative affect (0.286) (see Figure 4). These findings indicate that body-wandering is linked to a distinct neural connectivity profile, characterized by a pattern of increased thalamo-cortical coupling interconnecting interoceptive and somatomotor brain regions.

Examining the connectivity edges with the highest canonical loadings, we found that the strongest connections were between somatomotor/interoceptive regions and subcortical areas. Specifically, these included connections from the right thalamus and right caudate to the bilateral precentral gyrus (primary motor cortex, as defined by the Juelich Histological Atlas) and bilateral postcentral gyrus (primary somatosensory cortex), with top 1% absolute loadings ranging from 0.558 to 0.703. Additionally, we observed high-loading edges connecting the right paracingulate gyrus and bilateral postcentral gyrus, notably with a loading of 0.679 for the right postcentral gyrus (see Supplementary Table 5 for detailed connectivity loadings). We also assessed the connectivity degree among the top 1% highest loading connections, measured by the total number of above-threshold edges for each node (cite). The right thalamus had the highest degree (53 edges), followed by the right postcentral gyrus (24), left thalamus (22), right caudate (22), left putamen (21), and left postcentral gyrus (18) (see Supplementary Table 6).

To better understand the specificity of these effects, we explored how individual differences in the neural variate identified by the CCA relate to body-wandering and cognitive-wandering averages. To do so, we correlated each participant's weighting on the behavioural dimension of the CCA mode (i.e., the combined body/cognitive mind-wandering CCA variate) with their body-wandering and cognitive-wandering averages, we found a strong correlation with the body-wandering average ($rs = 0.481$, $pFDR < 0.001$) and a weaker correlation with the cognitive-wandering average ($rs = 0.152$, $pFDR < 0.001$). This indicates that the latent CCA variate is more closely associated with body-wandering than with cognitive-wandering, reinforcing the

idea that the neural connectivity patterns identified are specifically linked to embodied thought processes.

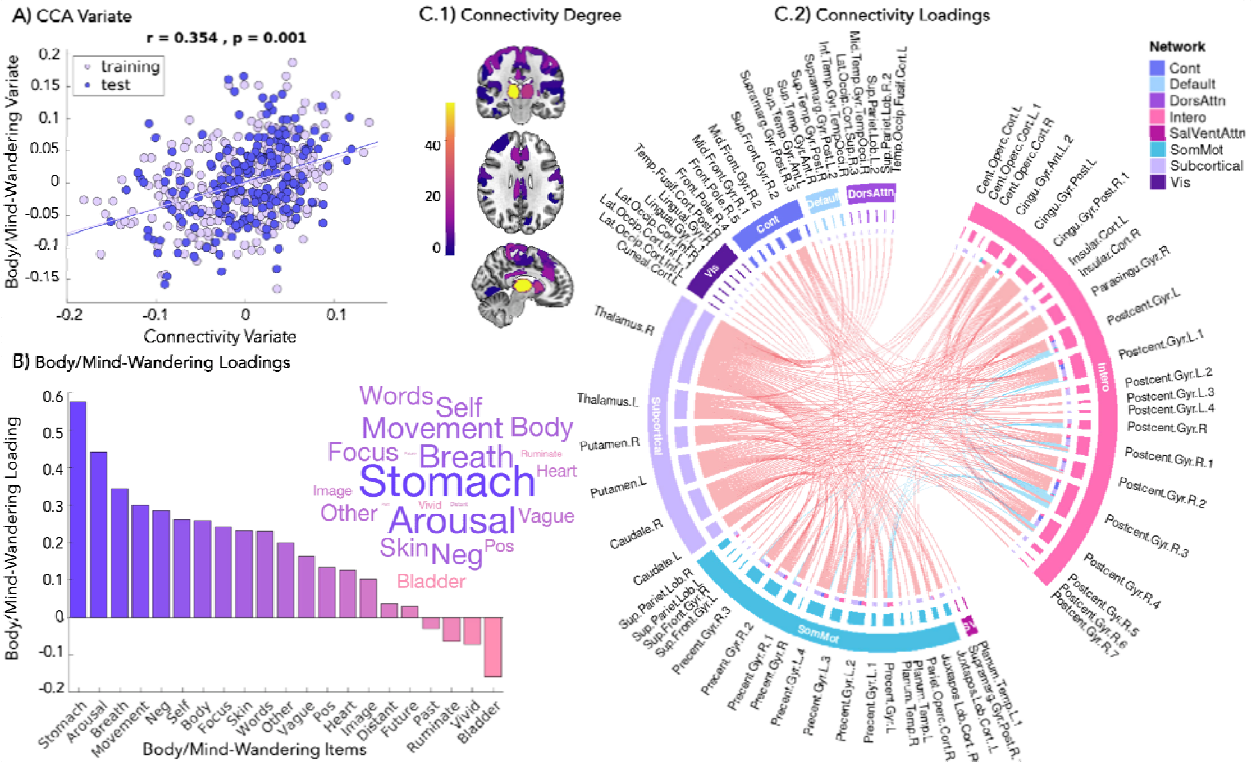

Figure 4: Functional connectivity fingerprint of embodied mind-wandering via Canonical Correlation Analysis.

(A) Canonical Correlation Analysis relationship describing a cross-validated maximally correlated pattern of functional connectivity with the embodied mind-wandering structure. (B) The CCA loadings (structure correlations: Pearson's correlations between mind-wandering item-level ratings and the mind-wandering canonical variate) denoting the pattern of mind-wandering data that is maximally correlated with the functional connectivity canonical variate. High positive loadings are shown for mind-wandering of the stomach, arousal, breath, movement and negative affective content. (C) The functional connectivity CCA loadings (structure correlations), thresholded at the top 1% of absolute loadings (> absolute 0.558). (C.1) Of the top 1% connectivity loadings, the summed total edges for each region (i.e., connectivity degree): highest include right thalamus, right postcentral gyrus, left thalamus, right caudate, left putamen, and the left postcentral gyrus (plotted on a standard mni152 brain template using MRIcroGL at the following MNI coordinates: 8, -20, 28). (C.2) Chord plot of the top 1% of connectivity edge CCA loadings representing high connectivity between the interoceptive-allostatic network and somatomotor network with subcortical regions.

Gradient map association

To situate the body-wandering brain variate within the greater topological hierarchy of the brain, we next applied a gradient-based analysis. To do so we investigated the association of the body-wandering CCA result with respect to previously defined gradient brain variation dimensions validated from the Human Connectome Projects resting state connectivity data (Margulies et al., 2016). These modes of brain variation are often referred to as gradients: Gradient-1 (Association to Primary cortex), Gradient-2 (Visual to Motor cortex), Gradient-3 (Frontoparietal to Default Mode Networks) and Gradient-4 (Dorsal Attention Network/Visual to Default Mode Networks), and Gradient-5 (Lateral Default Mode to Primary sensory cortex) (Margulies et al., 2016; Wallace et al., 2024). Thus, we implemented spin-tests to statistically determine the relationship of the top 1% brain regions from the CCA result to the gradient brain variation dimensions. We did this by averaging the gradient values across the top 1% brain parcels from the CCA, and consequently determined the likelihood of a value of this magnitude occurring by chance via a spin-test null distribution with 2500 permutations (Alexander-Bloch et al., 2018).

The top loading brain regions from the body-wandering CCA were significantly associated with Gradient-1 ($p < .001$). Gradient-2 did not pass multiple-comparisons correction ($p = .048$, Bonferroni $a = 0.01$), while Gradients 3-5 were also not significant (smallest $p = .189$). The negative loading sensory side of Gradient-1 was found in bilateral somatosensory and motor regions (i.e., postcentral and precentral gyrus), while the positive loading association side of Gradient-1 was demonstrated in right frontal (i.e., right superior and middle frontal gyrus) and bilateral cingulate regions (see Figure 5). The negative loading motor side of Gradient-2 was localised to bilateral motor regions (i.e., precentral gyrus), while the positive loading visual side of Gradient-2 was shown in broad visual areas (i.e., left cuneal cortex, bilateral lingual gyrus, and bilateral lateral occipital cortex), although not significant once controlling for multiple-comparisons.

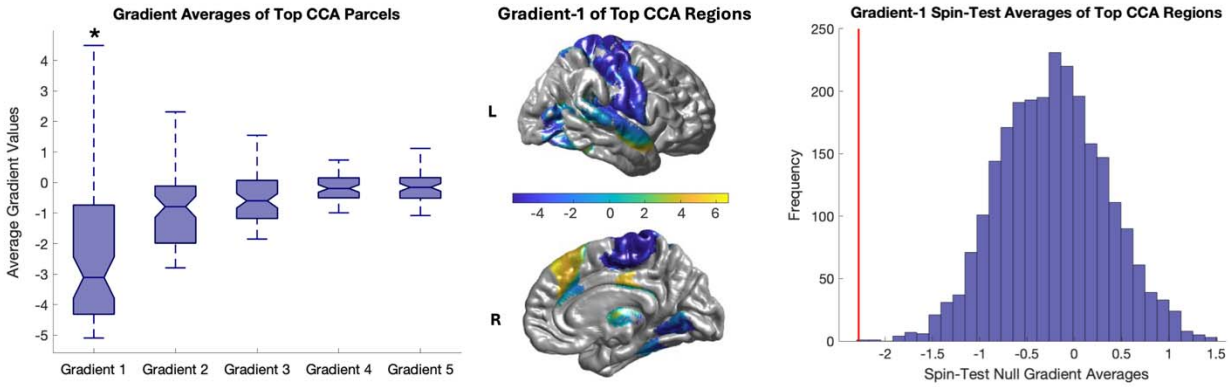

Figure 5: Relationship of the top 1% of brain regions from the body-wandering CCA with gradient brain variation dimensions via spin permutation tests. (Left) Boxplots of average values from each gradient atlas (Margulies et al., 2016) for each of the top 1% CCA brain parcels

(asterisks mark whether significant via a spin-test null distribution with 2500 permutations). (Middle) The top 1% of CCA brain regions coloured by the Gradient-1 atlas, including high negative loadings for somatosensory and motor regions (postcentral and precentral gyrus), and high positive loadings for right frontal (i.e., right superior and middle frontal gyrus) and bilateral cingulate regions. (Right) Spin-test result for the average Gradient-1 atlas value across the top 1% of brain parcels (red vertical line), in comparison to the average values determined from a spin-test null distribution with 2500 permutations (Alexander-Bloch et al., 2018).

Discussion

Our study set out to understand the possibility that our ongoing thoughts may have an embodied or interoceptive component, neglected from previous mind-wandering accounts. Using a novel experience sampling (i.e., MDIES) battery that accounted for the possibility that our thoughts relate to somatic and visceral sensations, we found that body-wandering was distinguishable from more cognitive aspects of ongoing thought in terms of their associations with emotional content, physiological responses, and mental health. For example, body-wandering was associated with a pattern of more negative thoughts, reduced ADHD symptoms, and higher arousal reflected in increased heart rate, breathing depth, breathing variability, and gastric motility, as well as reduced parasympathetic cardiac activity. In the opposing direction, cognitive features of experience (i.e., cognitive-wandering) were linked to more positive thoughts, but also more trait depression symptoms, and reduced arousal reflected in decreased breathing depth and gastric motility, as well as increased parasympathetic cardiac activity. We also revealed that individual differences in brain connectivity relating to body-wandering patterns involved interoceptive, somatomotor, and subcortical regions. Together these findings suggest that there is a distinct and separable mode of ongoing cognition that is coloured by our internal bodily processes and is likely made possible through the process of introspection.

The entanglement of emotion with embodied experiences has been discussed for centuries (Damasio et al., 1997; James, 1884; Niedenthal, 2007; Schachter & Singer, 1962), with some describing the perception and interpretation of interoceptive bodily changes as integral to emotion. This aligns with our observation of increased body-wandering with more negative thoughts. Compatibly, prior research indicated that individuals with heightened perception of their internal bodily signals report more intense emotions (Pollatos et al., 2007; Schandry, 1981; Wiens et al., 2000). However, a recent comprehensive meta-analysis uncovered a nuanced and heterogeneous relationship of interoception and emotion intensity, indicating a significant association primarily when experimentally induced via emotional images or facial expressions (Parrinello et al., 2022). In contrast, other emotion induction methods such as social exclusion, negative feedback, or during rest, reveal no differences in objective interoception (Parrinello et al., 2022; Zamariola, Frost, et al., 2019). Interestingly, even without objective interoception differences, individuals with a higher subjective sense of perceiving their internal signals experience more negative emotions post social exclusion or negative feedback (Zamariola,

Luminet, et al., 2019). Therefore, the role of awareness of bodily signals and emotions is complex and potentially context-dependent, and is further exacerbated by challenges in assessing interoception (Desmedt et al., 2018; Ring & Brener, 2018; Zamariola et al., 2018). Our results highlight that in a potentially anxiety-inducing MRI-scanner environment, interoceptive body-wandering has negative emotional impacts, aligning with research on anxiety and bodily hyper-awareness (Dunn et al., 2010; Pollatos et al., 2007).

Despite identifying a negative emotional link with body-wandering, we discovered that individuals with elevated depression and ADHD symptoms engaged in less body-wandering. Although seemingly counter-intuitive, this observation is actually consistent with evidence of reduced interoceptive perception and heartbeat potential attenuation in depression (Dunn et al., 2007; Pollatos et al., 2009; Zhou et al., 2022) and ADHD (Kutscheidt et al., 2019). Some theoretical accounts describe both ADHD and depression as stemming from an underactive autonomic nervous system (Bellato et al., 2020, 2023; Dawson et al., 1977). This diminished autonomic reactivity to environmental stimuli could lead to increased cognitive-wandering, which is further corroborated by our findings of increased cognitive-wandering with lower arousal, and a greater presence of ADHD and depression symptoms. Indeed, we observe reduced arousal with increased cognitive-wandering, and enhanced arousal with body-wandering, reflected in our heart rate and heart rate variability metrics. It is therefore plausible that autonomic arousal inversely regulates body-wandering and cognitive-wandering, and dysfunction in this regulatory process may contribute to mental health symptoms. Importantly, arousal-mediated mind-wandering may influence state and trait emotional experiences differently. For example, body-wandering during heightened physiological arousal may trigger immediate negative emotions relevant to the present context, but it may also reduce attention lapses into broader cognitive-wandering, such as thoughts about temporal and social aspects of life. This pattern has been previously related to depression (Hoffmann et al., 2016; Poerio et al., 2013; Smallwood & O'Connor, 2011), and is supported by our findings of increased temporal-oriented thoughts in individuals with elevated depression symptoms.

Our study makes an important theoretical contribution to our understanding of the brain mechanism behind specific patterns of ongoing thought by highlighting the role sensory regions make to our conscious experience. Prior studies have highlighted that patterns of self-generated episodic thought patterns are often linked to a decoupling between regions within association cortices, particularly the default mode network from the dorsal attention network, a process that is supported by regions of dorsolateral prefrontal cortex, (Hardikar et al., 2024; Turnbull et al., 2019). Other studies have shown that regions of visual and auditory cortex support situations when our ongoing thoughts are coupled to events in the outside world such as during movie watching (Wallace et al., 2024). In contrast, we observe that our ongoing thoughts can be spontaneously directed to bodily sensations, and that increased body-wandering is associated with a functional connectivity profile that is commonly seen in interoceptive studies (Azzalini et al., 2019; Engelen et al., 2023; Khalsa et al., 2009) consisting of regions within viscero-sensory

cortices (i.e., somatomotor and interoceptive networks) and subcortical regions (i.e., thalamus, caudate, putamen). This observation is important because it extends our understanding of the neural regions that support different types of ongoing thought patterns. In particular, it suggests that sometimes our spontaneous thoughts can be influenced by the state of our body, possibly through the process of interoception.

It is important to note that our study retrospectively probed body-wandering content with the aim of mapping their neural, psychological, and physiological fingerprints. Thus, future research should aim to qualitatively dissect the contents of interoceptive body-wandering in more detail. For example, it would be valuable to determine whether these thoughts pertain to specific interoceptive sensations, or broader body-related themes, such as body-image, recalling the enjoyment of a meal, or feeling one's heart race during an emotional moment. Additionally, using smartphone-based ecological momentary assessments (Mulholland et al., 2023) to capture real-time introspective contributions in daily life could provide insight into the contexts where body-wandering occurs most frequently.

In conclusion, we are the first to characterise the neural, psychological, and physiological fingerprints of body-wandering. We observe a distinct pattern of ongoing thought that focused on bodily sensations that was dissociable from the cognitive features of experience that make up the bulk of studies of mind-wandering. This distinction spanned affective, physiological, and psychological dimensions, and highlighted an important contribution of somatomotor and interoceptive networks in shaping the stream of ongoing conscious experiences.

Materials and methods

Participants

We recruited 566 (360 females, 205 males, 1 other gender) participants (median age = 24, age range = 18-56) as part of the Visceral Mind Project, a large-scale neuroimaging study conducted at the Centre of Functionally Integrative Neuroscience, Aarhus University. We acquired participants via the SONA system participation pool at Aarhus University, or via local advertisements on posters and social media. Participants were provided with hourly compensation for their participation in the study. Participants had normal or corrected-to-normal vision and were fluent in Danish or English. Furthermore, we only included participants compatible with MRI scanning (e.g., not pregnant or breastfeeding, no metal implants, claustrophobia). Participants took part in multiple tasks, MRI scans, physiological recordings and completed mental health and lifestyle inventories. In this study, we focus on the retrospective mind-wandering responses, as well as the resting state fMRI data, physiological recordings (photoplethysmography, respiration belt, electrogastrography), and mental health assessments on depression and ADHD symptoms. The local Region Midtjylland Ethics Committee granted approval for the study and all participants provided informed consent. The study was conducted in accordance with the Declaration of Helsinki. 536 participants completed the post-resting state

mind-wandering (338 females, 197 males, 1 other gender, median age = 24, age range = 18-56). After the removal of poor-quality fMRI data (see f/MRI preprocessing Methods for Quality Control procedures), a total of 489 full-dataset participants were included in the functional connectivity CCA analysis with body-wandering (311 females, 178 males, median age = 24, age range = 18-56) (see Supplementary Figure 16 for a full flow-chart of sample sizes).

Multidimensional interoceptive experience sampling (MDIES)

We developed a multidimensional interoceptive experience sampling (MDIES) scale to retrospectively measure participants' ongoing thoughts following the resting state scan. The scale consisted of an expanded version of the traditional multidimensional experiential sampling (mDES) technique by including items on interoceptive and somatic content (F. J. M. Ruby et al., 2013; Smallwood et al., 2016), for a total of 22 items. Participants responded to all questions using a visual analogue scale, on a range of 0 to 100 (see Table 1). The presentation order of probe items was randomised across participants.

Table 1: ***Multidimensional interoceptive experience sampling (MDIES) items asked after resting state fMRI.***

Dimension	Item	Scale=0	Scale=100
Future	My thoughts involved future events.	Not at all	Completely
Past	My thoughts involved past events.	Not at all	Completely
Self	My thoughts involved myself.	Not at all	Completely
Other	My thoughts involved other people.	Not at all	Completely
Positive	My thoughts were positive.	Not at all	Completely
Negative	My thoughts were negative.	Not at all	Completely
Words	My thoughts were in the form of words.	Not at all	Completely
Vivid	My thoughts were vivid as if I was there.	Not at all	Completely
Vague	My thoughts were detailed and specific.	Not at all	Completely
Spontaneous	My thoughts were:	Spontaneous	Deliberate

Focus	My thoughts were focused.	Not at all	Completely
Ruminate	My thoughts were repetitive.	Not at all	Completely
Temporal distance	My thoughts were related to:	The here and now	A more distant time
Images	My thoughts were in the form of images.	Not at all	Completely
Arousal	In general, I felt more:	Sleepy	Alert
Body	My thoughts were about my body.	Not at all	Completely
Breath	My thoughts were about my breathing.	Not at all	Completely
Heart	My thoughts were about my heartbeat.	Not at all	Completely
Movement	My thoughts were about moving.	Not at all	Completely
Bladder	My thoughts were about my bladder.	Not at all	Completely
Skin	My thoughts were about my skin.	Not at all	Completely
Stomach	My thoughts were about my stomach.	Not at all	Completely

Resting-state fMRI acquisition

We acquired anatomical and resting state fMRI data using a 3 T MRI scanner (Siemens Prisma) with a 32-channel head coil. We positioned small cushions around the head to minimise head movement. The participants wore earplugs and were instructed to keep as still as possible during the scans. The resting state scan included 600 volumes over 14 minutes using a T2*-weighted echo-planar imaging (EPI) multiband accelerated sequence (TR = 1400 ms, TE = 29.6 ms, voxel size = 1.79 x 1.79 x 1.80 mm). An acceleration factor of 4 was used in the slice direction along with GRAPPA in-plane acceleration factor of 2, and a flip-angle of 75°. A set of high-resolution whole brain T1-weighted anatomical images (0.9 mm^3 isotropic) were acquired using an MP-RAGE sequence (repetition time□=□2.2 s, echo time□=□2.51 ms, matrix size□=□256□×□256 x 192□voxels, flip angle□=□8°, AP acquisition direction). To increase comfort, all participants were instructed to use the bathroom just before scanning.

f/MRI Preprocessing

All fMRI data were preprocessed using fMRIPrep 22.1.1 (Esteban et al., 2019, 2022), built on Nipype 1.8.5 (Gorgolewski et al., 2018). The anatomical T1-weighted image was corrected for

intensity non-uniformity using N4BiasFieldCorrection (Tustison et al., 2010) and ANTs 2.3.3, (Avants et al., 2008), skull-stripped, and segmented into gray matter, white matter, and cerebrospinal fluid using FAST (FSL 6.0.5.1) (Zhang et al., 2001). Brain surfaces were reconstructed using recon-all with FreeSurfer 7.2.0 (Dale et al., 1999), and the brain mask was estimated to reconcile ANTs-derived and FreeSurfer-derived cortical segmentations (Klein et al., 2017). Spatial normalization was performed using nonlinear registration to MNI152NLin2009cAsym and MNI152NLin6Asym templates via antsRegistration (ANTs 2.3.3).

For functional preprocessing, the resting-state fMRI were slice-time corrected using 3dTshift from AFNI ((Cox & Hyde, 1997), motion-corrected using MCFLIRT (FSL 6.0.5.1) (Jenkinson et al., 2002), and co-registered to the T1w reference using bbregister (FreeSurfer) (Greve & Fischl, 2009). Confounds including framewise displacement, DVARS, and CompCor components (combined anatomical and temporal) were computed (Behzadi et al., 2007; Jenkinson et al., 2002; Power et al., 2014). Motion estimates were expanded with temporal derivatives and quadratic terms. Functional data were resampled to native space and standard space (MNI152NLin2009cAsym) using a single interpolation step to minimize smoothing effects. Resampling to the fsaverage surface was also performed (Glasser et al., 2013). Poor quality fMRI data was excluded if any brain abnormalities were present, framewise displacement > 0.25, parts of brain image cut, unfinished recordings, or large motion artefacts in T1.

Functional connectivity analysis utilized the Schaefer atlas (200 cortical regions) with an additional 16 subcortical regions, and connectivity was estimated using Nilearn's "ConnectivityMeasure" function, generating full 216-node correlation matrices. We low pass filtered at 0.08. Additional nuisance variable noise regression was performed using 24 motion parameters, noise signals from white matter and cerebral spinal fluid, six aCompCor 'anat_combined' parameters, and a high pass filter (Abraham et al., 2014; Behzadi et al., 2007).

For further details on the fMRI preprocessing workflow, please refer to the Supplementary Material.

Physiological measurements

Physiological recording acquisition

We simultaneously recorded physiological measurements (photoplethysmography, respiratory breathing belt, and electrogastrography) during resting-state fMRI. The photoplethysmography was recorded on the right cheek via a Sentec Digital Monitoring system for the first data collection cohort at 1000 Hz (208 participants) and on the left index/middle finger via the MRI scanner for the second cohort at 200 Hz (325 participants). We obtained respiratory recordings using a Siemens respiratory cushion and belt system. The first data collection cohort was recorded via a Brain Vision ExG system at 1000 Hz (208 participants), while the second cohort was recorded via an MRI scanner at 50 Hz (316 participants). For the EGG recordings, we

cleaned the abdomen and applied abrasive gel to remove dead skin and improve the signal-to-noise ratio. Three electrogastrography recording montages (1, 3 or 6 bipolar channels) were implemented using a Brain Vision MRI-compatible ExG system and amplifier. All ExG physiological recordings were acquired with a sampling rate of 1000 Hz, a low-pass filter of 1000 Hz, and no high-pass filter (DC recordings). EGG was recorded at a 0.5 μV/bit resolution, and +/- 16.384 mV range, while photoplethysmography and respiratory recordings were acquired at 152.6 μV/bit resolution, and +/- 5000 mV range.

Cardiac preprocessing

R-peaks were identified from the cardiac recordings using the python package ‘systole’ using the ‘rolling_average_ppg’ method, while correcting for clipping artefacts in the second cohort’s data using a threshold of 950’000 and a cubic spline interpolation method. All the detected R-peaks were visually inspected and manually corrected, if necessary, as well as unintelligible segments marked and discarded. We excluded participants with less than 2 minutes of continuous cardiac recording. We computed heart rate as the mean of the beats per minute, while heart rate variability was defined as the root mean square of successive differences of the R-R intervals in milliseconds (RMSSD). Heart rate variability in the frequency domain was calculated by estimating a Welch power spectrum density. The high frequency power in normalised units was defined as high frequency power (0.15 Hz - 0.4 Hz), divided by high and low frequency combined (0.04 Hz - 0.4 Hz), multiplied by 100 (Legrand & Allen, 2022).

Respiratory preprocessing

To address occasional missing samples from the scanner respiratory recordings, we performed linear interpolation on the second cohort's data. We excluded respiratory data if the recording was less than 7 minutes. We preprocessed the respiratory recordings by Butterworth filtering with a cutoff of 1 and an order of 4. We computed the z-score of the respiratory recordings for peak (i.e., inhalation) and trough (i.e., exhalation) detection. For inhalation peak detection, we employed the 'find_peaks' function from the ‘scipy.signal’ Python library, setting distance to 1, prominence to 0.6, and width to 2. We defined exhalation troughs as the minimum points between the identified peaks. We visually inspected peak and trough detection, manually correcting, if necessary, by adding missing peaks/troughs or removing incorrect ones.

Breath duration was calculated as the time between peaks in seconds, inspiration depth as the difference in signal strength between the peak and the preceding trough (i.e., peak minus previous trough), and expiration depth as the difference in signal strength between the peak and the subsequent trough (i.e., peak minus following trough). We computed the mean and standard deviation of these single peak-to-peak and trough measurements, yielding the following respiratory metrics: mean breath duration, breath duration standard deviation, mean breath depth, and breath depth standard deviation (averaging/standard deviation across inspiration and

expiration depths). Additionally, we defined the respiration rate as the number of breaths per minute.

Gastric preprocessing

The EGG data was first demeaned and downsampled from 1000 Hz to 10 Hz, followed by computing the power spectrum using a Hanning-tapered fast Fourier transform incorporating 1000 seconds of zero-padding in 200-second data segments with 75% overlap. For each participant, we selected the bipolar EGG channel that showed the most prominent peak within the normogastric range (0.033-0.066 Hz). Specifically, two independent researchers conducted peak selection by visually inspecting each channel to identify the EGG channel with the highest normogastric power peak, without large artefacts and with power above 5 µv2. Peak quality was rated as 'excellent' for Gaussian-like peaks (n=184) and 'good' for shoulder-like peaks (n=81); those not meeting these standards were deemed 'poor quality' (n=115) and excluded. The selected EGG channel was then bandpass filtered, centred at the individual peak frequency (filter width of ±0.015 Hz, filter order of 5 or 1470 samples).

From the computed EGG power spectra, we quantified the following normogastric EGG metrics: peak frequency, maximum power and proportion of power. Specifically, within the normogastric frequency range (0.033-0.067 Hz/2-4 cpm/15-30 seconds), we stored the peak frequency and maximum power. Furthermore, we computed the proportion of normogastric power as the sum of the normogastric power divided by the sum of the power in all gastric frequencies (including bradygastric, normogastric and tachygastric frequencies: 0.02-0.17 Hz/1-10 cpm/6-60 seconds).

Physiological metric processing

We log transformed the following physiological metrics to ensure approximate normal distributions: RMSSD, LF/HF ratio, breathing duration variability, maximum power in normogastria. Furthermore, we removed outliers from all physiological metrics as 3 standard deviations from the mean.

Mental health assessment

We explored the mental health relationship of embodied and cognitive mind-wandering, specifically with individual differences in ADHD and depression symptoms. ADHD symptoms were assessed via the Adult ADHD Self-Report Scale (ASRS) using combined sum scores from both part A and part B (Kessler et al., 2005), while depression symptoms were examined via sum scores from the Major Depression Inventory (MDI) (with the highest score taken from 8a and 8b, 9a and 9b, 10a and 10b) (Bech et al., 2015). Psychological symptom assessment was completed online before attending the fMRI scan. We deliberately included participants ranging from subclinical symptom variation to symptom severity passing diagnostic clinical cut-offs. Specifically, 19% passed clinical thresholds for an ADHD diagnosis (binarised ASRS part A

sum-score >=4), 2% for high levels of depression (MDI sum-score >30), 5% for moderate depression (MDI sum-score 26-30), and 6% for mild depression (MDI sum-score 21-25) (Kessler et al., 2005; Olsen et al., 2003). We log transformed the MDI sum scores to ensure an approximate normal distribution. Furthermore, we removed outliers from both the ASRS and MDI scores as 3 standard deviations from the mean.

Data analysis

The mind-wandering item-level and mind-wandering average-level Wilcoxon signed-rank tests, partial correlations (controlling for age, gender, and BMI), and backward stepwise multiple linear regressions were completed in JASP 0.18.3. The FDR-corrected mind-wandering item-level cross correlations, the FDR-corrected mind-wandering average-level correlations with mental health symptoms and physiological metrics, and the item-level network analysis was conducted in Rstudio 2023.03.0. Finally, the CCA of mind-wandering with functional connectivity and the gradient-based analysis was completed in Matlab 9.10.0.1710957 (R2021a), using the CCA-PLS toolbox (Mihalik et al., 2022).

Item cross correlation

We conducted exploratory Spearman's cross-correlations on the MDIES item rating responses themselves, with p-values corrected for multiple comparisons using the false discovery rate. We also estimated partial correlations controlling for age, gender and body mass index.

Mind-wandering summaries

As we expanded upon the mind-wandering multidimensional experiential sampling approach (mDES) to include interoceptive/embodied items (MDIES), we summarised these distinct components of the scale to represent individual differences in overall body-wandering and cognitive-wandering experiences. Previous literature demonstrated clusters of cognitive components of mind-wandering incorporating socio-temporal dimensions (Linz et al., 2021; F. J. Ruby et al., 2013; F. J. M. Ruby et al., 2013). Therefore, we averaged across these cognitive socio-temporal aspects of mind-wandering (Future, Past, Self, Other) to represent cognitive-wandering. Furthermore, we defined body-wandering by averaging across embodied and interoceptive mind-wandering items (Body, Breath, Heart, Movement, Bladder, Skin, Stomach). Finally, we computed the difference of negative and positive affective ratings (Neg - Pos) to characterise overall negative affective mind-wandering. We compared the prevalence of body-wandering with cognitive mind-wandering via a paired-sample t-test.

Psychological network analysis

To conduct network analysis of body and mind-wandering items, we applied the 'bootnet' R package to represent the 21 MDIES items as nodes, with edges signifying partial correlation coefficients (Epskamp et al., 2018). We employed the EBICglasso method for network estimation, which incorporates a graphical least absolute shrinkage and selection operator (glasso) that shrinks edge weights towards zero, fostering a sparse network and reducing spurious edges. An Extended Bayesian Information Criterion (EBIC) is used to set a regularisation tuning parameter for estimating a weighted network.

To determine the influence of each node on the network, we computed four centrality indices: strength, betweenness, closeness, and expected influence (Opsahl et al., 2010). Strength signifies the node's direct connections to other nodes (absolute sum of nodes direct edge weights). Betweenness measures how often a node appears in the shortest path between other nodes (sum of number of times a node is in the middle of two other nodes), indicating its importance in connecting other nodes. Closeness represents nodes with the most indirect connections (sum of nodes distance: inverse of the sum of inverted edge weights). Lastly, expected influence is calculated as the sum of edge weights including both positive and negative weights, signifying the anticipated impact on activating/deactivating other nodes (Robinaugh et al., 2016).

We assessed the network's accuracy and stability through edge-weight accuracy and centrality stability evaluations. First, we estimated 95% confidence intervals using non-parametric bootstrapping with 2,500 bootstraps for edge-weight accuracy. We then evaluated centrality stability by conducting case-dropping subset bootstrapping with 2,500 bootstraps and determining the consistency of centrality indices in each subset (Epskamp et al., 2018). Finally, we tested for significant differences across centrality indices and edges.

We investigated community structures of nodes identified via a Spinglass modularity-based community detection algorithm (Reichardt & Bornholdt, 2006). This algorithm is suited for networks with both positive and negative edge weights.

Physiological and psychological fingerprints

We investigated the physiological and psychological fingerprints of average body-wandering, average cognitive-wandering, and negative affective mind-wandering via false-discovery rate corrected Spearman’s correlation matrices. Additional partial correlations controlled for age, gender, and BMI. Post-hoc correlations were performed with individual mind-wandering items with any significant psychological score or physiological metric from the averaged mind-wandering correlations. Finally, we conducted backward stepwise multiple linear regressions to determine significant psychological and physiological predictors of body vs cognitive-wandering.

Canonical correlation analysis

In this study, we used the CCA-PLS toolbox to fit cross-validated Canonical Correlation Analysis (CCA) models relating whole-brain functional connectivity matrices to individual body-wandering and cognitive-wandering (MDIES) items. The CCA-PLS toolbox is a MATLAB-based software designed for investigating multivariate associations between multiple modalities of data, such as brain imaging and behavioural measures (Mihalik et al., 2022). Specifically, CCA aims to find linear combinations of each multidimensional variable (i.e., canonical variates, which are weighted sums: connectivity (i.e., V = X * B) and body/cognitive-wandering (i.e., U = Y * A)) that are maximally correlated with each other, but uncorrelated with all other combinations (X and Y represent the inputted data, while A and B represent the canonical weights/vectors) (Linke et al., 2021; Mihalik et al., 2022). The toolbox incorporates various CCA/PLS models, including the cross-validated and optimised PCA-CCA techniques applied here.

We began by preprocessing the whole-brain functional connectivity matrices and individual MDIES items, ensuring that each dataset was standardised to have zero mean and unit variance. Furthermore, we regressed nuisance covariates (i.e., gender, age, bmi, data collection cohort) from both the connectivity and MDIES item variables. Subsequently, we applied the cross-validated CCA approach within the predictive framework (i.e., machine learning) provided by the CCA-PLS toolbox. This predictive approach involved randomly splitting the data into an optimization/training set (i.e., 60% of the overall data) and a holdout/test set (i.e., 40% of the overall data) 5 times (i.e., 5-fold cross-validation). These optimization and holdout sets are known as the 'outer data splits', used for statistical inference (i.e., determining the number of significant associative CCA effects/modes). The p-values were calculated via permutation testing (i.e., 1000 permutations), as the fraction of the shuffled permuted out-of-sample correlations exceeding the out-of-sample correlation in the non-permuted holdout set. Because we implemented 5 holdout sets, the p-value for each holdout set was Bonferroni corrected (i.e., a = 0.05/5 = 0.01). An associative CCA effect was considered significant if the p-value was significant in at least one of the holdout sets. If a significant associative CCA effect was found, the CCA iteratively removes the effect from the data via deflation and repeats this approach to find orthogonal CCA associative effects.

Furthermore, because we conducted PCA before CCA (to reduce the connectivity data and body/cognitive mind-wandering item data dimensions), we further divided the optimization set into a training set (i.e., 60% of the optimization set) and a validation set (i.e., 40% of the optimization set) 5 times (i.e., 5-fold hyperparameter optimization). These 'inner data splits' were used to select the optimal hyperparameters (i.e., number of PCA components for each dataset) by maximising the average out-of-sample correlation in the validation sets (i.e., model generalizability). In addition to evaluating model generalizability via the predictive approach, we assessed the stability of the CCA models by measuring the average similarity of weights across

different training sets. Furthermore, we assessed the robustness (i.e., number of significant data splits) of the CCA model (80%).

To visualise the results, we plotted the maximally correlated canonical variate via a scatter plot, and the connectivity and body/cognitive-wandering structure correlations (i.e., Pearson's correlations between inputted variables and respective canonical variates) using a chord plot, and bar plot/word cloud, respectively. Bar plots and word clouds were used to display the individual mind-wandering item loadings (structure correlations of raw items with the mind-wandering variate), while chord plots provided a graphical representation of the connections between brain regions and their corresponding loadings (structure correlations of raw functional connectivity data with the functional connectivity variate), thresholded at showing the top 99th percentile of the connectivity loadings. To visualise the brain networks contributing to the CCA result, we organised top connectivity loadings in the chord plot according to yeo-7 networks (Yeo et al., 2011). In addition, recently there has been interest in the properties of an 'interoceptive-allostatic network' (Kleckner et al., 2017). To define this network we reviewed the neuroanatomy and functional imaging literature on interoception and defined cortical regions in the interoceptive network as follows: insular cortex, cingulate cortex, frontal orbital cortex, frontal medial cortex, postcentral gyrus (primary somatosensory cortex), and central opercular cortex (secondary somatosensory cortex) (Azzalini et al., 2019; Barrett & Simmons, 2015; Craig, 2002; Engelen et al., 2023; Khalsa et al., 2009; Kleckner et al., 2017). Furthermore, we illustrated the highest contributing nodes by summing the amount of edge connections above the 99th percentile cutoff for each node. This was plotted on a standard mni152 brain template using MRIcroGL at the following MNI coordinates: 8, -20, 28. These visualisations allowed for a clearer understanding of the associations between the whole-brain functional connectivity matrices and individual body/cognitive-wandering items, highlighting the key brain-behaviour relationships identified by our cross-validated CCA model.

Gradient map association

We investigated the localisation of the body-wandering CCA result in relation to five brain variation gradient maps from the Human Connectome Project resting connectivity data (Margulies et al., 2016). These gradients (five cortical and subcortical surface atlases) were extracted from Neurovault (https://neurovault.org/collections/1598/). The combined 200-cortical-region Schaefer-16-subcortical-region atlas was converted to surface space using the freesurfer function '*mri_vol2surf*' (this removed the bilateral caudate as these deep subcortical regions were not represented in surface space). For each of the five gradient maps, we averaged the gradient values of the top CCA brain parcels (parcels which passed the top 1% threshold of the connectivity CCA loadings) and generated a null distribution with 2500 permutations via a spin-test which shuffles the gradient values. The p-values were generated by comparing the overall gradient average across the top CCA brain regions, with the 2500 null averages generated from

the spin-test. The five p-values computed from repeating this process for each of the five gradient atlases, were Bonferroni corrected (i.e., $a = 0.05/5 = 0.01$).

Data availability

Deidentified participant data and scripts implemented in this paper are available here: https://github.com/embodied-computation-group/body_wandering_CCA_

Acknowledgements

This research is financially supported by a Lundbeckfonden Fellowship (R272-2017-4345) and a European Research Council Grant (ERC-2020-StG-948788) awarded to MGA. FF is supported by a European Research Council Grant (ERC-2020-StG-948838) and a Lundbeckfonden Experiment Grant (R436-2023-991). The funding sources were not involved in the study design, collection, analysis, interpretation, or writing of the manuscript.

Author contributions

LB analysed the data, interpreted the results, and wrote the manuscript, NN collected the data, provided conceptual advice and contributed towards preprocessing of neuroimaging data, MB contibuted towards the preprocessing of the physiological data, MN collected the data, FF provided conceptual advice and edited the manuscript, JS provided conceptual advice, analysis supervision, and wrote the manuscript, MA provided supervision, conceptual advice, and wrote the manuscript.

Competing interests

All authors declare no conflicts of interest.

Materials and correspondence

Leah Banellis: leahbanellis@cfin.au.dk.

References

Abraham, A., Pedregosa, F., Eickenberg, M., Gervais, P., Mueller, A., Kossaifi, J., Gramfort, A., Thirion, B., & Varoquaux, G. (2014). Machine learning for neuroimaging with scikit-learn. *Frontiers in Neuroinformatics*, *8*. https://www.frontiersin.org/articles/10.3389/fninf.2014.00014

Alexander-Bloch, A. F., Shou, H., Liu, S., Satterthwaite, T. D., Glahn, D. C., Shinohara, R. T., Vandekar, S. N., & Raznahan, A. (2018). On testing for spatial correspondence between maps of human brain structure and function. *NeuroImage*, *178*, 540–551. https://doi.org/10.1016/j.neuroimage.2018.05.070

Avants, B. B., Epstein, C. L., Grossman, M., & Gee, J. C. (2008). Symmetric diffeomorphic image registration with cross-correlation: Evaluating automated labeling of elderly and neurodegenerative brain. *Medical Image Analysis*, *12*(1), 26–41. https://doi.org/10.1016/j.media.2007.06.004

Azzalini, D., Rebollo, I., & Tallon-Baudry, C. (2019). Visceral Signals Shape Brain Dynamics and Cognition. *Trends in Cognitive Sciences*, *23*(6), 488–509. https://doi.org/10.1016/j.tics.2019.03.007

Babo-Rebelo, M., Buot, A., & Tallon-Baudry, C. (2019). Neural responses to heartbeats distinguish self from other during imagination. *NeuroImage*, *191*, 10–20. https://doi.org/10.1016/j.neuroimage.2019.02.012

Babo-Rebelo, M., Richter, C. G., & Tallon-Baudry, C. (2016). Neural Responses to Heartbeats in the Default Network Encode the Self in Spontaneous Thoughts. *Journal of Neuroscience*, *36*(30), 7829–7840. https://doi.org/10.1523/JNEUROSCI.0262-16.2016

Babo-Rebelo, M., Wolpert, N., Adam, C., Hasboun, D., & Tallon-Baudry, C. (2016). Is the cardiac monitoring function related to the self in both the default network and right anterior insula? *Philosophical Transactions of the Royal Society B: Biological Sciences*, *371*(1708), 20160004. https://doi.org/10.1098/rstb.2016.0004

Barrett, L. F., & Simmons, W. K. (2015). Interoceptive predictions in the brain. *Nature Reviews Neuroscience*, *16*(7), 419–429. https://doi.org/10.1038/nrn3950

Bech, P., Timmerby, N., Martiny, K., Lunde, M., & Soendergaard, S. (2015). Psychometric evaluation of the Major Depression Inventory (MDI) as depression severity scale using the LEAD (Longitudinal Expert Assessment of All Data) as index of validity. *BMC Psychiatry*, *15*(1), 190. https://doi.org/10.1186/s12888-015-0529-3

Behzadi, Y., Restom, K., Liau, J., & Liu, T. T. (2007). A component based noise correction method (CompCor) for BOLD and perfusion based fMRI. *NeuroImage*, *37*(1), 90–101. https://doi.org/10.1016/j.neuroimage.2007.04.042

Bellato, A., Arora, I., Hollis, C., & Groom, M. J. (2020). Is autonomic nervous system function atypical in attention deficit hyperactivity disorder (ADHD)? A systematic review of the evidence. *Neuroscience & Biobehavioral Reviews*, *108*, 182–206. https://doi.org/10.1016/j.neubiorev.2019.11.001

Bellato, A., Wiersema, J. R., & Groom, M. J. (2023). Autonomic Nervous System Functioning in ADHD. In J. L. Matson (Ed.), *Clinical Handbook of ADHD Assessment and Treatment Across the Lifespan* (pp. 37–75). Springer International Publishing. https://doi.org/10.1007/978-3-031-41709-2_3

Biederman, J., Lanier, J., DiSalvo, M., Noyes, E., Fried, R., Woodworth, K. Y., Biederman, I., & Faraone, S. V. (2019). Clinical correlates of mind wandering in adults with ADHD. *Journal of Psychiatric Research*, *117*, 15–23. https://doi.org/10.1016/j.jpsychires.2019.06.012

Bozhilova, N. S., Michelini, G., Kuntsi, J., & Asherson, P. (2018). Mind wandering perspective on attention-deficit/hyperactivity disorder. *Neuroscience & Biobehavioral Reviews*, *92*, 464–476. https://doi.org/10.1016/j.neubiorev.2018.07.010

Christoff, K., Gordon, A. M., Smallwood, J., Smith, R., & Schooler, J. W. (2009). Experience sampling during fMRI reveals default network and executive system contributions to mind wandering. *Proceedings of the National Academy of Sciences of the United States of America*, *106*(21), 8719–8724. https://doi.org/10.1073/pnas.0900234106

Christoff, K., Irving, Z. C., Fox, K. C. R., Spreng, R. N., & Andrews-Hanna, J. R. (2016). Mind-wandering as spontaneous thought: A dynamic framework. *Nature Reviews Neuroscience*, *17*(11), 718–731. https://doi.org/10.1038/nrn.2016.113

Cox, R. W., & Hyde, J. S. (1997). Software tools for analysis and visualization of fMRI data. *NMR in Biomedicine*, *10*(4–5), 171–178. https://doi.org/10.1002/(SICI)1099-1492(199706/08)10:4/5<171::AID-NBM453>3.0.CO;2-L

Craig, A. D. (2002). How do you feel? Interoception: the sense of the physiological condition of the body. *Nature Reviews Neuroscience*, *3*(8), 655–666. https://doi.org/10.1038/nrn894

Critchley, H. D., & Garfinkel, S. N. (2017). Interoception and emotion. *Current Opinion in Psychology*, *17*, 7–14. https://doi.org/10.1016/j.copsyc.2017.04.020

Dale, A. M., Fischl, B., & Sereno, M. I. (1999). Cortical Surface-Based Analysis: I. Segmentation and Surface Reconstruction. *NeuroImage*, *9*(2), 179–194. https://doi.org/10.1006/nimg.1998.0395

Damasio, A. R., Everitt, B. J., Bishop, D., Roberts, A. C., Robbins, T. W., & Weiskrantz, L. (1997). The somatic marker hypothesis and the possible functions of the prefrontal cortex. *Philosophical Transactions of the Royal Society of London. Series B: Biological Sciences*, *351*(1346), 1413–1420. https://doi.org/10.1098/rstb.1996.0125

Dawson, M. E., Schell, A. M., & Catania, J. J. (1977). Autonomic Correlates of Depression and Clinical Improvement Following Electroconvulsive Shock Therapy. *Psychophysiology*, *14*(6), 569–578. https://doi.org/10.1111/j.1469-8986.1977.tb01201.x

Desmedt, O., Luminet, O., & Corneille, O. (2018). The heartbeat counting task largely involves non-interoceptive processes: Evidence from both the original and an adapted counting task. *Biological Psychology*, *138*, 185–188. https://doi.org/10.1016/j.biopsycho.2018.09.004

Dunn, B. D., Dalgleish, T., Ogilvie, A. D., & Lawrence, A. D. (2007). Heartbeat perception in depression. *Behaviour Research and Therapy*, *45*(8), 1921–1930. https://doi.org/10.1016/j.brat.2006.09.008

Dunn, B. D., Stefanovitch, I., Evans, D., Oliver, C., Hawkins, A., & Dalgleish, T. (2010). Can you feel the beat? Interoceptive awareness is an interactive function of anxiety- and depression-specific symptom dimensions. *Behaviour Research and Therapy*, *48*(11), 1133–1138. https://doi.org/10.1016/j.brat.2010.07.006

Engelen, T., Solcà, M., & Tallon-Baudry, C. (2023). Interoceptive rhythms in the brain. *Nature Neuroscience*, *26*(10), Article 10. https://doi.org/10.1038/s41593-023-01425-1

Epskamp, S., Borsboom, D., & Fried, E. I. (2018). Estimating psychological networks and their accuracy: A tutorial paper. *Behavior Research Methods*, *50*(1), 195–212. https://doi.org/10.3758/s13428-017-0862-1

Esteban, O., Markiewicz, C. J., Blair, R. W., Moodie, C. A., Isik, A. I., Erramuzpe, A., Kent, J. D., Goncalves, M., DuPre, E., Snyder, M., Oya, H., Ghosh, S. S., Wright, J., Durnez, J., Poldrack, R. A., & Gorgolewski, K. J. (2019). fMRIPrep: A robust preprocessing pipeline for functional MRI. *Nature Methods*, *16*(1), Article 1. https://doi.org/10.1038/s41592-018-0235-4

Esteban, O., Markiewicz, C. J., Burns, C., Goncalves, M., Jarecka, D., Ziegler, E., Berleant, S., Ellis, D. G., Pinsard, B., Madison, C., Waskom, M., Notter, M. P., Clark, D., Manhães-Savio, A., Clark, D., Jordan, K., Dayan, M., Halchenko, Y. O., Loney, F., … Ghosh, S. (2022). *nipy/nipype: 1.8.3* [Computer software]. Zenodo. https://doi.org/10.5281/zenodo.6834519

Fox, K. C. R., Spreng, R. N., Ellamil, M., Andrews-Hanna, J. R., & Christoff, K. (2015). The wandering brain: Meta-analysis of functional neuroimaging studies of mind-wandering and related spontaneous thought processes. *NeuroImage*, *111*, 611–621. https://doi.org/10.1016/j.neuroimage.2015.02.039

Gable, S. L., Hopper, E. A., & Schooler, J. W. (2019). When the Muses Strike: Creative Ideas of Physicists and Writers Routinely Occur During Mind Wandering. *Psychological Science*, *30*(3), 396–404. https://doi.org/10.1177/0956797618820626

Glasser, M. F., Sotiropoulos, S. N., Wilson, J. A., Coalson, T. S., Fischl, B., Andersson, J. L., Xu, J., Jbabdi, S., Webster, M., Polimeni, J. R., Van Essen, D. C., & Jenkinson, M. (2013). The minimal preprocessing pipelines for the Human Connectome Project. *NeuroImage*, *80*, 105–124. https://doi.org/10.1016/j.neuroimage.2013.04.127

Gorgolewski, K., Ziegler, E., Ellis, D. G., Notter, M. P., & Perkins, L. N. (2018). *Nipype*. [Computer software].

Greicius, M. D., Krasnow, B., Reiss, A. L., & Menon, V. (2003). Functional connectivity in the resting brain: A network analysis of the default mode hypothesis. *Proceedings of the National Academy of Sciences*, *100*(1), 253–258. https://doi.org/10.1073/pnas.0135058100

Greve, D. N., & Fischl, B. (2009). Accurate and robust brain image alignment using boundary-based registration. *NeuroImage*, *48*(1), 63–72. https://doi.org/10.1016/j.neuroimage.2009.06.060

Hardikar, S., Mckeown, B., Schaare, H. L., Wallace, R., Xu, T., Lauckner, M. E., Valk, S. L., Margulies, D. S., Turnbull, A., Bernhardt, B., Wael, R. V. de, Villringer, A., & Smallwood, J. (2024). Macro-scale patterns in functional connectivity associated with ongoing thought patterns and dispositional traits. *eLife*, *13*. https://doi.org/10.7554/eLife.93689.2

Hoffmann, F., Banzhaf, C., Kanske, P., Bermpohl, F., & Singer, T. (2016). Where the depressed mind wanders: Self-generated thought patterns as assessed through experience sampling as a state marker of depression. *Journal of Affective Disorders*, *198*, 127–134. https://doi.org/10.1016/j.jad.2016.03.005

James, W. (1884). What is an Emotion? *Mind*, *9*(34), 188–205. JSTOR.

Jenkinson, M., Bannister, P., Brady, M., & Smith, S. (2002). Improved Optimization for the Robust and Accurate Linear Registration and Motion Correction of Brain Images. *NeuroImage*, *17*(2), 825–841. https://doi.org/10.1006/nimg.2002.1132

Kessler, R. C., Adler, L., Ames, M., Demler, O., Faraone, S., Hiripi, E., Howes, M. J., Jin, R., Secnik, K., Spencer, T., Ustun, T. B., & Walters, E. E. (2005). The World Health Organization adult ADHD self-report scale (ASRS): A short screening scale for use in the general population. *Psychological Medicine*, *35*(2), 245–256. https://doi.org/10.1017/S0033291704002892

Khalsa, S. S., Adolphs, R., Cameron, O. G., Critchley, H. D., Davenport, P. W., Feinstein, J. S., Feusner, J. D., Garfinkel, S. N., Lane, R. D., Mehling, W. E., Meuret, A. E., Nemeroff, C. B., Oppenheimer, S., Petzschner, F. H., Pollatos, O., Rhudy, J. L., Schramm, L. P., Simmons, W. K., Stein, M. B., … Zucker, N. (2018). Interoception and Mental Health: A Roadmap. *Biological Psychiatry: Cognitive Neuroscience and Neuroimaging*, *3*(6), 501–513. https://doi.org/10.1016/j.bpsc.2017.12.004

Khalsa, S. S., Rudrauf, D., Feinstein, J. S., & Tranel, D. (2009). The pathways of interoceptive awareness. *Nature Neuroscience*, *12*(12), Article 12. https://doi.org/10.1038/nn.2411

Killingsworth, M., & Gilbert, D. (2010). A Wandering Mind Is an Unhappy Mind. *Science*, *330*. https://www.science.org/doi/full/10.1126/science.1192439

Kleckner, I. R., Zhang, J., Touroutoglou, A., Chanes, L., Xia, C., Simmons, W. K., Quigley, K. S., Dickerson, B. C., & Feldman Barrett, L. (2017). Evidence for a large-scale brain system supporting allostasis and interoception in humans. *Nature Human Behaviour*, *1*(5), 0069. https://doi.org/10.1038/s41562-017-0069

Klein, A., Ghosh, S. S., Bao, F. S., Giard, J., Häme, Y., Stavsky, E., Lee, N., Rossa, B., Reuter, M., Neto, E. C., & Keshavan, A. (2017). Mindboggling morphometry of human brains. *PLOS Computational Biology*, *13*(2), e1005350. https://doi.org/10.1371/journal.pcbi.1005350

Konu, D., Turnbull, A., Karapanagiotidis, T., Wang, H.-T., Brown, L. R., Jefferies, E., & Smallwood, J. (2020). A role for the ventromedial prefrontal cortex in self-generated episodic social cognition. *NeuroImage*, *218*, 116977. https://doi.org/10.1016/j.neuroimage.2020.116977

Kutscheidt, K., Dresler, T., Hudak, J., Barth, B., Blume, F., Ethofer, T., Fallgatter, A. J., & Ehlis, A.-C. (2019). Interoceptive awareness in patients with attention-deficit/hyperactivity disorder (ADHD).

ADHD Attention Deficit and Hyperactivity Disorders, *11*(4), 395–401. https://doi.org/10.1007/s12402-019-00299-3

Lanier, J., Noyes, E., & Biederman, J. (2021). Mind Wandering (Internal Distractibility) in ADHD: A Literature Review. *Journal of Attention Disorders*, *25*(6), 885–890. https://doi.org/10.1177/1087054719865781

Legrand, N., & Allen, M. (2022). Systole: A python package for cardiac signal synchrony and analysis. *Journal of Open Source Software*, *7*(69), 3832.

Linke, J. O., Abend, R., Kircanski, K., Clayton, M., Stavish, C., Benson, B. E., Brotman, M. A., Renaud, O., Smith, S. M., Nichols, T. E., Leibenluft, E., Winkler, A. M., & Pine, D. S. (2021). Shared and Anxiety-Specific Pediatric Psychopathology Dimensions Manifest Distributed Neural Correlates. *Biological Psychiatry*, *89*(6), 579–587. https://doi.org/10.1016/j.biopsych.2020.10.018

Linz, R., Pauly, R., Smallwood, J., & Engert, V. (2021). Mind-wandering content differentially translates from lab to daily life and relates to subjective stress experience. *Psychological Research*, *85*(2), 649–659. https://doi.org/10.1007/s00426-019-01275-2

Margulies, D. S., Ghosh, S. S., Goulas, A., Falkiewicz, M., Huntenburg, J. M., Langs, G., Bezgin, G., Eickhoff, S. B., Castellanos, F. X., Petrides, M., Jefferies, E., & Smallwood, J. (2016). Situating the default-mode network along a principal gradient of macroscale cortical organization. *Proceedings of the National Academy of Sciences*, *113*(44), 12574–12579. https://doi.org/10.1073/pnas.1608282113

Martella, D., Aldunate, N., Fuentes, L. J., & Sánchez-Pérez, N. (2020). Arousal and Executive Alterations in Attention Deficit Hyperactivity Disorder (ADHD). *Frontiers in Psychology*, *11*. https://www.frontiersin.org/journals/psychology/articles/10.3389/fpsyg.2020.01991

Mckeown, B., Poerio, G. L., Strawson, W. H., Martinon, L. M., Riby, L. M., Jefferies, E., McCall, C., & Smallwood, J. (2021). The impact of social isolation and changes in work patterns on ongoing thought during the first COVID-19 lockdown in the United Kingdom. *Proceedings of the National Academy of Sciences of the United States of America*, *118*(40), e2102565118. https://doi.org/10.1073/pnas.2102565118

Mckeown, B., Strawson, W. H., Zhang, M., Turnbull, A., Konu, D., Karapanagiotidis, T., Wang, H.-T., Leech, R., Xu, T., Hardikar, S., Bernhardt, B., Margulies, D., Jefferies, E., Wammes, J., & Smallwood, J. (2023). Experience sampling reveals the role that covert goal states play in task-relevant behavior. *Scientific Reports*, *13*(1), 21710. https://doi.org/10.1038/s41598-023-48857-0

Mihalik, A., Chapman, J., Adams, R. A., Winter, N. R., Ferreira, F. S., Shawe-Taylor, J., & Mourão-Miranda, J. (2022). Canonical Correlation Analysis and Partial Least Squares for Identifying Brain–Behavior Associations: A Tutorial and a Comparative Study. *Biological Psychiatry: Cognitive Neuroscience and Neuroimaging*, *7*(11), 1055–1067. https://doi.org/10.1016/j.bpsc.2022.07.012

Mulholland, B., Goodall-Halliwell, I., Wallace, R., Chitiz, L., Mckeown, B., Rastan, A., Poerio, G. L., Leech, R., Turnbull, A., Klein, A., Milham, M., Wammes, J. D., Jefferies, E., & Smallwood, J.

(2023). Patterns of ongoing thought in the real world. *Consciousness and Cognition*, *114*, 103530. https://doi.org/10.1016/j.concog.2023.103530

Niedenthal, P. M. (2007). Embodying Emotion. *Science*, *316*(5827), 1002–1005. https://doi.org/10.1126/science.1136930

Olsen, L. R., Jensen, D. V., Noerholm, V., Martiny, K., & Bech, P. (2003). The internal and external validity of the Major Depression Inventory in measuring severity of depressive states. *Psychological Medicine*, *33*(2), 351–356. https://doi.org/10.1017/S0033291702006724

Opsahl, T., Agneessens, F., & Skvoretz, J. (2010). Node centrality in weighted networks: Generalizing degree and shortest paths. *Social Networks*, *32*(3), 245–251. https://doi.org/10.1016/j.socnet.2010.03.006

Park, H.-D., Bernasconi, F., Salomon, R., Tallon-Baudry, C., Spinelli, L., Seeck, M., Schaller, K., & Blanke, O. (2018). Neural Sources and Underlying Mechanisms of Neural Responses to Heartbeats, and their Role in Bodily Self-consciousness: An Intracranial EEG Study. *Cerebral Cortex*, *28*(7), 2351–2364. https://doi.org/10.1093/cercor/bhx136

Parrinello, N., Napieralski, J., Gerlach, A. L., & Pohl, A. (2022). Embodied feelings–A meta-analysis on the relation of emotion intensity perception and interoceptive accuracy. *Physiology & Behavior*, *254*, 113904. https://doi.org/10.1016/j.physbeh.2022.113904

Poerio, G. L., Totterdell, P., & Miles, E. (2013). Mind-wandering and negative mood: Does one thing really lead to another? *Consciousness and Cognition*, *22*(4), 1412–1421. https://doi.org/10.1016/j.concog.2013.09.012

Pollatos, O., Traut-Mattausch, E., & Schandry, R. (2009). Differential effects of anxiety and depression on interoceptive accuracy. *Depression and Anxiety*, *26*(2), 167–173. https://doi.org/10.1002/da.20504

Pollatos, O., Traut-Mattausch, E., Schroeder, H., & Schandry, R. (2007). Interoceptive awareness mediates the relationship between anxiety and the intensity of unpleasant feelings. *Journal of Anxiety Disorders*, *21*(7), 931–943. https://doi.org/10.1016/j.janxdis.2006.12.004

Power, J. D., Mitra, A., Laumann, T. O., Snyder, A. Z., Schlaggar, B. L., & Petersen, S. E. (2014). Methods to detect, characterize, and remove motion artifact in resting state fMRI. *NeuroImage*, *84*, 320–341. https://doi.org/10.1016/j.neuroimage.2013.08.048

Raichle, M. E., MacLeod, A. M., Snyder, A. Z., Powers, W. J., Gusnard, D. A., & Shulman, G. L. (2001). A default mode of brain function. *Proceedings of the National Academy of Sciences*, *98*(2), 676–682. https://doi.org/10.1073/pnas.98.2.676

Reichardt, J., & Bornholdt, S. (2006). Statistical mechanics of community detection. *Physical Review. E, Statistical, Nonlinear, and Soft Matter Physics*, *74*(1 Pt 2), 016110. https://doi.org/10.1103/PhysRevE.74.016110

Ring, C., & Brener, J. (2018). Heartbeat counting is unrelated to heartbeat detection: A comparison of methods to quantify interoception. *Psychophysiology*, *55*(9), e13084. https://doi.org/10.1111/psyp.13084

Robe, A., Dobrean, A., Cristea, I. A., Păsărelu, C. R., & Predescu, E. (2019). Attention-deficit/hyperactivity disorder and task-related heart rate variability: A systematic review and meta-analysis. *Neuroscience & Biobehavioral Reviews*, *99*, 11–22. https://doi.org/10.1016/j.neubiorev.2019.01.022

Robinaugh, D. J., Millner, A. J., & McNally, R. J. (2016). Identifying Highly Influential Nodes in the Complicated Grief Network. *Journal of Abnormal Psychology*, *125*(6), 747–757. https://doi.org/10.1037/abn0000181

Ruby, F. J. M., Smallwood, J., Engen, H., & Singer, T. (2013). How Self-Generated Thought Shapes Mood—The Relation between Mind-Wandering and Mood Depends on the Socio-Temporal Content of Thoughts. *PLoS ONE*, *8*(10), e77554. https://doi.org/10.1371/journal.pone.0077554

Ruby, F. J., Smallwood, J., Sackur, J., & Singer, T. (2013). Is self-generated thought a means of social problem solving? *Frontiers in Psychology*, *4*. https://www.frontiersin.org/journals/psychology/articles/10.3389/fpsyg.2013.00962

Schachter, S., & Singer, J. (1962). Cognitive, social, and physiological determinants of emotional state. *Psychological Review*, *69*, 379–399. https://doi.org/10.1037/h0046234

Schandry, R. (1981). Heart Beat Perception and Emotional Experience. *Psychophysiology*, *18*(4), 483–488. https://doi.org/10.1111/j.1469-8986.1981.tb02486.x

Smallwood, J., Karapanagiotidis, T., Ruby, F., Medea, B., de Caso, I., Konishi, M., Wang, H.-T., Hallam, G., Margulies, D. S., & Jefferies, E. (2016). Representing Representation: Integration between the Temporal Lobe and the Posterior Cingulate Influences the Content and Form of Spontaneous Thought. *PLOS ONE*, *11*(4), e0152272. https://doi.org/10.1371/journal.pone.0152272

Smallwood, J., & O'Connor, R. C. (2011). Imprisoned by the past: Unhappy moods lead to a retrospective bias to mind wandering. *Cognition and Emotion*, *25*(8), 1481–1490. https://doi.org/10.1080/02699931.2010.545263

Smallwood, J., & Schooler, J. W. (2015). The Science of Mind Wandering: Empirically Navigating the Stream of Consciousness. *Annual Review of Psychology*, *66*(1), 487–518. https://doi.org/10.1146/annurev-psych-010814-015331

Smallwood, J., Turnbull, A., Wang, H., Ho, N. S. P., Poerio, G. L., Karapanagiotidis, T., Konu, D., Mckeown, B., Zhang, M., Murphy, C., Vatansever, D., Bzdok, D., Konishi, M., Leech, R., Seli, P., Schooler, J. W., Bernhardt, B., Margulies, D. S., & Jefferies, E. (2021). The neural correlates of ongoing conscious thought. *iScience*, *24*(3). https://doi.org/10.1016/j.isci.2021.102132

Turnbull, A., Wang, H. T., Murphy, C., Ho, N. S. P., Wang, X., Sormaz, M., Karapanagiotidis, T., Leech, R. M., Bernhardt, B., Margulies, D. S., Vatansever, D., Jefferies, E., & Smallwood, J. (2019). Left dorsolateral prefrontal cortex supports context-dependent prioritisation of off-task thought. *Nature Communications*, *10*(1), 3816. https://doi.org/10.1038/s41467-019-11764-y

Tustison, N. J., Avants, B. B., Cook, P. A., Zheng, Y., Egan, A., Yushkevich, P. A., & Gee, J. C. (2010). N4ITK: Improved N3 Bias Correction. *IEEE Transactions on Medical Imaging*, *29*(6), 1310–1320. IEEE Transactions on Medical Imaging. https://doi.org/10.1109/TMI.2010.2046908

Wallace, R. S., Mckeown, B., Goodall-Halliwell, I., Chitiz, L., Forest, P., Karapanagiotidis, T., Mulholland, B., Turnbull, A. G., Vanderwal, T., Hardikar, S., Alam, T. G., Bernhardt, B., Wang, H.-T., Strawson, W., Milham, M., Xu, T., Margulies, D., Poerio, G. L., Jefferies, E. S., … Smallwood, J. (2024). Mapping patterns of thought onto brain activity during movie-watching. *eLife*, *13*. https://doi.org/10.7554/eLife.97731.1

Wiens, S., Mezzacappa, E. S., & Katkin, E. S. (2000). Heartbeat detection and the experience of emotions. *Cognition and Emotion*, *14*(3), 417–427. https://doi.org/10.1080/026999300378905

Zamariola, G., Frost, N., Van Oost, A., Corneille, O., & Luminet, O. (2019). Relationship between interoception and emotion regulation: New evidence from mixed methods. *Journal of Affective Disorders*, *246*, 480–485. https://doi.org/10.1016/j.jad.2018.12.101

Zamariola, G., Luminet, O., Mierop, A., & Corneille, O. (2019). Does it help to feel your body? Evidence is inconclusive that interoceptive accuracy and sensibility help cope with negative experiences. *Cognition and Emotion*, *33*(8), 1627–1638. https://doi.org/10.1080/02699931.2019.1591345

Zamariola, G., Maurage, P., Luminet, O., & Corneille, O. (2018). Interoceptive accuracy scores from the heartbeat counting task are problematic: Evidence from simple bivariate correlations. *Biological Psychology*, *137*, 12–17. https://doi.org/10.1016/j.biopsycho.2018.06.006

Zhang, Y., Brady, M., & Smith, S. (2001). Segmentation of brain MR images through a hidden Markov random field model and the expectation-maximization algorithm. *IEEE Transactions on Medical Imaging*, *20*(1), 45–57. IEEE Transactions on Medical Imaging. https://doi.org/10.1109/42.906424

Zhou, H., Zou, H., Dai, Z., Zhao, S., Hua, L., Xia, Y., Han, Y., Yan, R., Tang, H., Huang, Y., Du, Y., Wang, X., Yao, Z., & Lu, Q. (2022). Interoception Dysfunction Contributes to the Negative Emotional Bias in Major Depressive Disorder. *Frontiers in Psychiatry*, *13*. https://www.frontiersin.org/journals/psychiatry/articles/10.3389/fpsyt.2022.874859

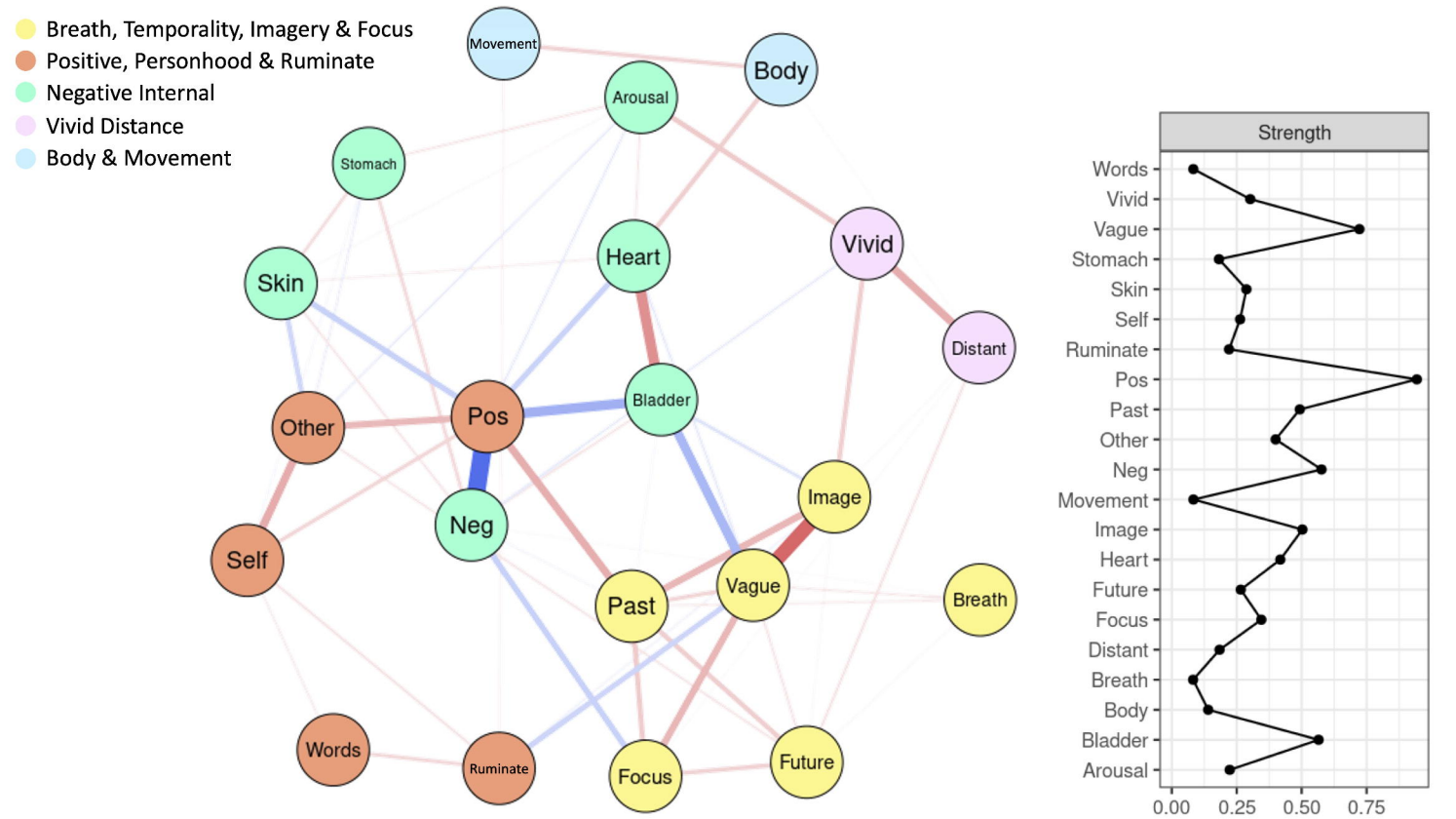
Breath, Temporality, Imagery & Focus
Positive, Personhood & Ruminate
Negative Internal
Vivid Distance
Body & Movement
Movement
Body
Arousal
Stomach
Vivid
Heart
Skin
Distant
Bladder
Other
Pos
Image
Neg
Self
Vague
Past
Breath
Words
Ruminate
Focus
Future
Strength
Words
Vivid
Vague
Stomach
Skin
Self
Ruminate
Pos
Past
Other
Neg
Movement
Image
Heart
Future
Focus
Distant
Breath
Body
Bladder
Arousal
0.00
0.25
0.50
0.75

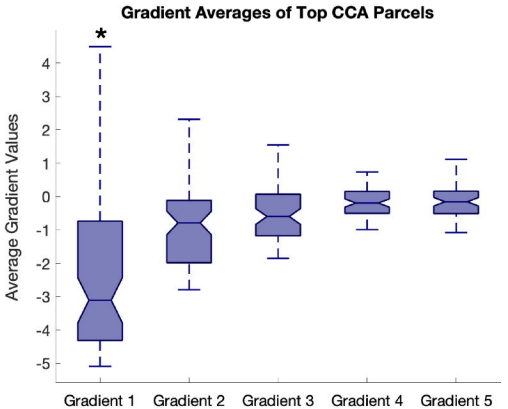
Gradient Averages of Top CCA Parcels
Average Gradient Values
*
4
3
2
1
0
-1
-2
-3
-4
-5
Gradient 1
Gradient 2
Gradient 3
Gradient 4
Gradient 5

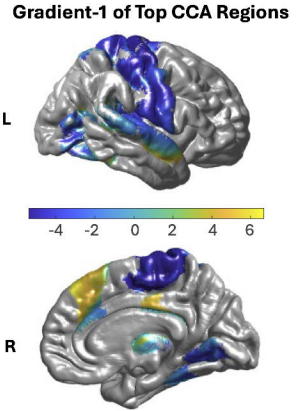
Gradient-1 of Top CCA Regions
L
R
-4
-2
0
2
4
6

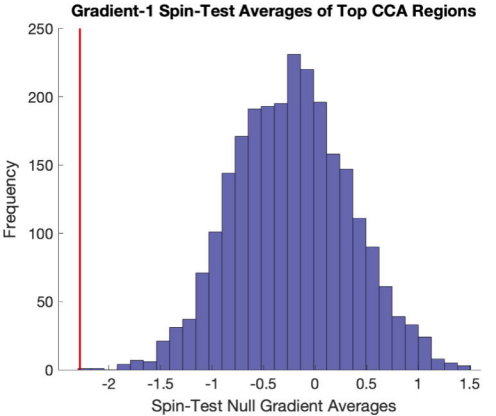
Gradient-1 Spin-Test Averages of Top CCA Regions
Frequency
250
200
150
100
50
0
-2
-1.5
-1
-0.5
0
0.5
1
1.5
Spin-Test Null Gradient Averages

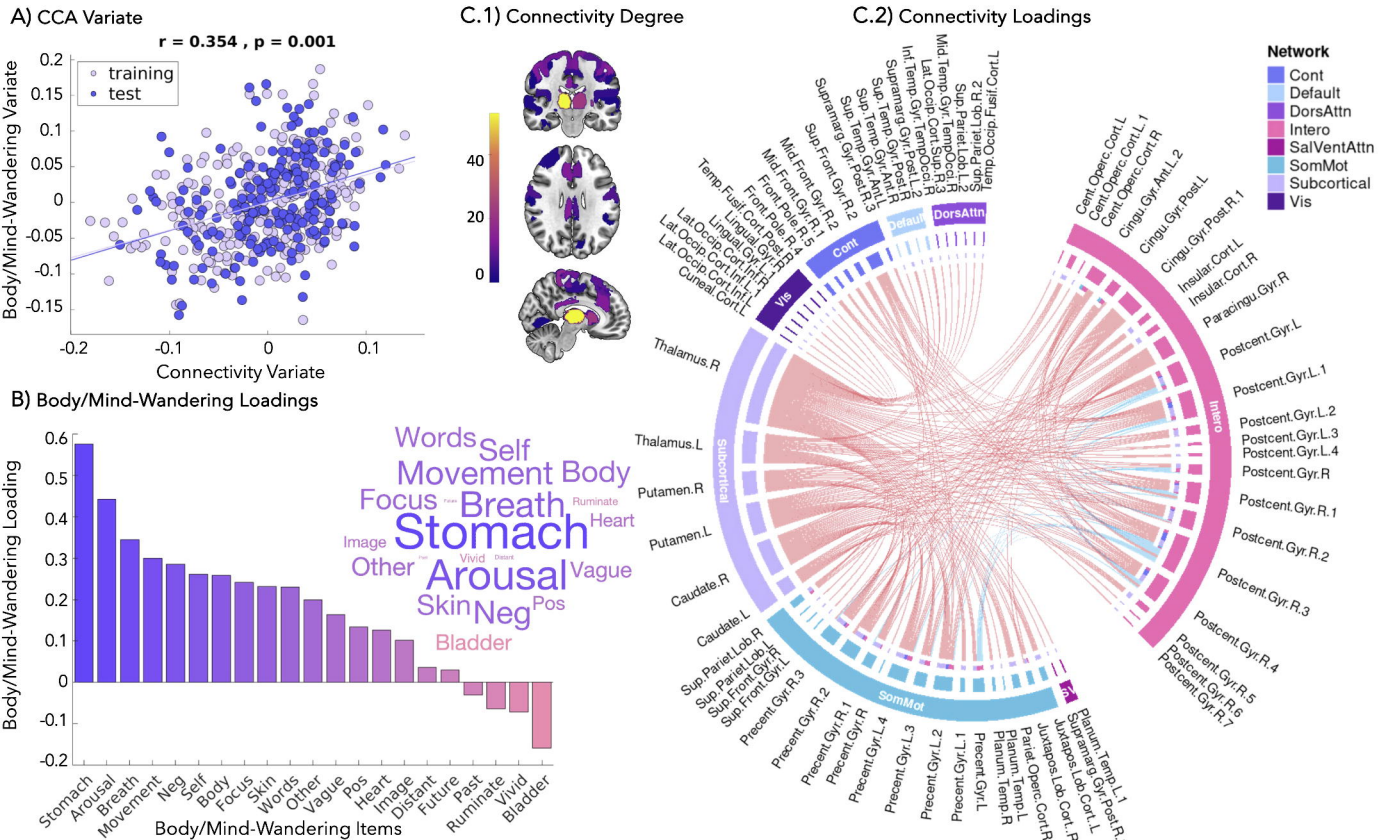
A) CCA Variate
r = 0.354 , p = 0.001
training
test
Body/Mind-Wandering Variate
Connectivity Variate
C.1) Connectivity Degree
40
20
0
C.2) Connectivity Loadings
Network
Cont
Default
DorsAttn
Intero
SalVentAttn
SomMot
Subcortical
Vis
B) Body/Mind-Wandering Loadings
Body/Mind-Wandering Loading
Body/Mind-Wandering Items
Stomach
Arousal
Breath
Movement
Neg
Self
Body
Focus
Skin
Words
Other
Vague
Pos
Heart
Image
Distant
Future
Past
Ruminate
Vivid
Bladder

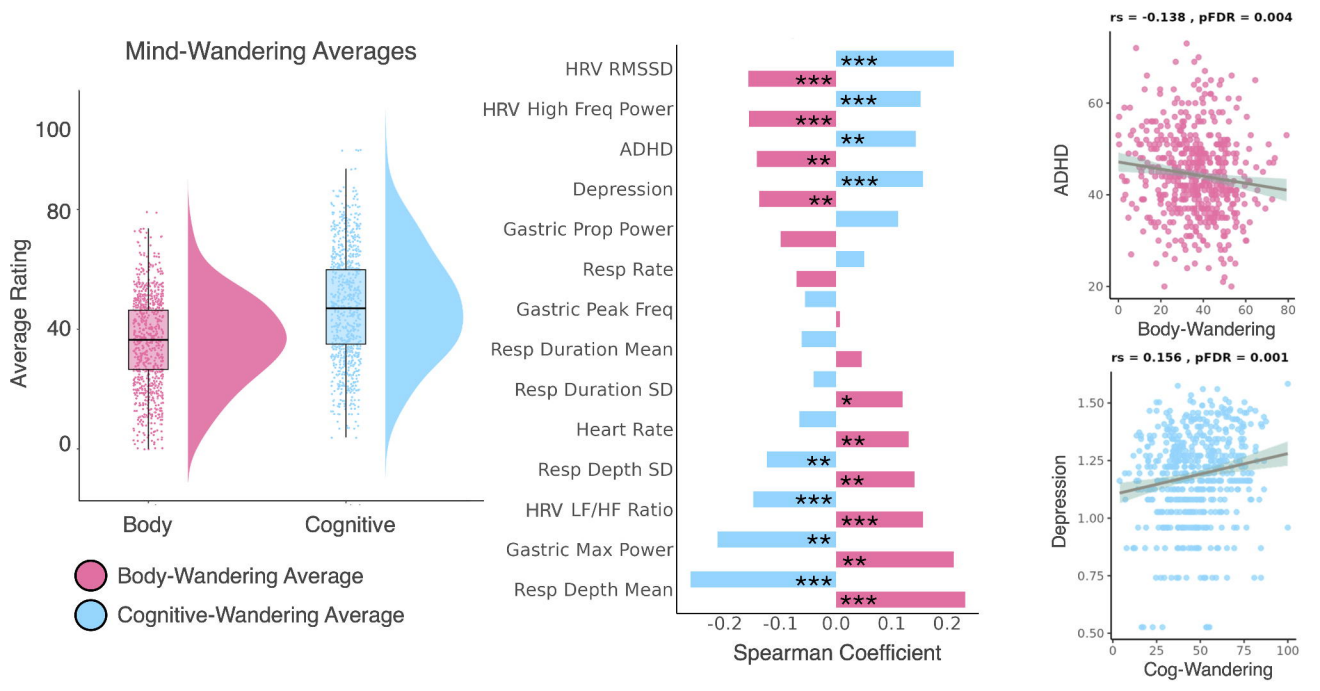
Mind-Wandering Averages
Average Rating
100
80
40
0
Body
Cognitive
Body-Wandering Average
Cognitive-Wandering Average
HRV RMSSD
HRV High Freq Power
ADHD
Depression
Gastric Prop Power
Resp Rate
Gastric Peak Freq
Resp Duration Mean
Resp Duration SD
Heart Rate
Resp Depth SD
HRV LF/HF Ratio
Gastric Max Power
Resp Depth Mean
-0.2
-0.1
0.0
0.1
0.2
Spearman Coefficient
rs = -0.138 , pFDR = 0.004
ADHD
Body-Wandering
rs = 0.156 , pFDR = 0.001
Depression
Cog-Wandering

MDIES Item
Self
Words
Vivid
Ruminate
Other
Image
Body
Vague
Pos
Distant
Future
Spontaneous
Movement
Breath
Focus
Past
Arousal
Heart
Neg
Stomach
Skin
Bladder
0
25
50
75
100
Rating
Body Items
Cognitive/Affective Items
Body Item
Bladder
Skin
Heart
Stomach
Arousal
Breath
Body
Movement
***
*
Affect Item
Neg
Pos
-0.3 -0.2 -0.1 0 0.1 0.2
Spearman Coefficient
Body Average
0.6
-0.3
Movement
Bladder
Words
Past
Skin
Pos
Vivid
Arousal
Heart
Other
Vague
Neg
Body
Image
Ruminate
Self
Breath
Spontaneous
Stomach
Cognitive Average
0.6
-0.3
Distant
Ruminate
Stomach
Words
Body
Heart
Past
Self
Bladder
Other
Arousal
Vague
Pos
Skin
Future
Breath
Focus
Image
Neg
Spontaneous
Negative Difference
0.6
-0.3
Stomach
Bladder
Self
Focus
Past
Neg
Skin
Other
Heart
Pos
Vivid
Ruminate